

Zeitschrift: IABSE publications = Mémoires AIPC = IVBH Abhandlungen
Band: 25 (1965)

Artikel: Three dimensional analysis of curved girder with thin-walled cross section
Autor: Konishi, Ichiro / Komatsu, Sadao
DOI: <https://doi.org/10.5169/seals-20353>

Nutzungsbedingungen

Die ETH-Bibliothek ist die Anbieterin der digitalisierten Zeitschriften auf E-Periodica. Sie besitzt keine Urheberrechte an den Zeitschriften und ist nicht verantwortlich für deren Inhalte. Die Rechte liegen in der Regel bei den Herausgebern beziehungsweise den externen Rechteinhabern. Das Veröffentlichen von Bildern in Print- und Online-Publikationen sowie auf Social Media-Kanälen oder Webseiten ist nur mit vorheriger Genehmigung der Rechteinhaber erlaubt. [Mehr erfahren](#)

Conditions d'utilisation

L'ETH Library est le fournisseur des revues numérisées. Elle ne détient aucun droit d'auteur sur les revues et n'est pas responsable de leur contenu. En règle générale, les droits sont détenus par les éditeurs ou les détenteurs de droits externes. La reproduction d'images dans des publications imprimées ou en ligne ainsi que sur des canaux de médias sociaux ou des sites web n'est autorisée qu'avec l'accord préalable des détenteurs des droits. [En savoir plus](#)

Terms of use

The ETH Library is the provider of the digitised journals. It does not own any copyrights to the journals and is not responsible for their content. The rights usually lie with the publishers or the external rights holders. Publishing images in print and online publications, as well as on social media channels or websites, is only permitted with the prior consent of the rights holders. [Find out more](#)

Download PDF: 21.06.2025

ETH-Bibliothek Zürich, E-Periodica, <https://www.e-periodica.ch>

Three Dimensional Analysis of Curved Girder with Thin-Walled Cross Section

Analyse tridimensionnelle des poutres courbes à parois minces

Dreidimensionale Untersuchung gekrümmter Träger mit dünnwandigem Querschnitt

ICHIRO KONISHI

Professor of Kyoto University

SADAO KOMATSU

Professor of Osaka University

Introduction

It is a well-known fact that the stress distribution along the height of the curved beam bent in its own plane will deviate from what calculated by the conventional bending stress formula for the straight beam.

Generally, the greater the curvature, the more the bending stress distribution at the radial section will deviate from that of straight beam. Based on this fact, it may be expected that, in the curved girder constructed out of thin-walled members, similar phenomena will occur under any external force.

So, just in the same correlation that the theory of curved beam bent in its own plane has been developed on the basis of primary bending theory for straight beam, it should be desired that fundamental theory for curved girder with thin-walled section, under arbitrary loading condition, will be systematically established by developing the present structural theory for straight thin-walled girder.

In this paper, much consideration is particularly given so as to clarify the effects of curvature on all quantitative relations such as displacement, stress distribution and so on.

So, generalized analysis has been conducted to obtain important formulae concerned with both stress resultants and deformation for seven fundamental conditions of deformation of free-free girder. Then the general formula for all kind of cross-sectional quantities have been derived.

Furthermore, paying careful attention to the bicoupling interrelation

between bending and torsion of whole structure, the solutions about the longitudinal variation of the stress resultants and deformations are induced in the simply supported as well as continuous curved girder subjected to several typical loading conditions.

I. Fundamental Theory of Curved Girder with Thin-Walled Section

1. Geometrical Properties of Cross-Section

Prior to the statical discussion on curved girder, the geometrical properties determined by the shape and dimensions of its cross section will be described. As shown in Fig. 1, a point C is arbitrarily selected at the cross section. Now, the center of curvature of the axis formed by connecting every point C in the longitudinal direction is designated as O . The girder is usually so constructed that each point on the cross section is arranged along the cylindrical surface, the axis of which passes through the center O .

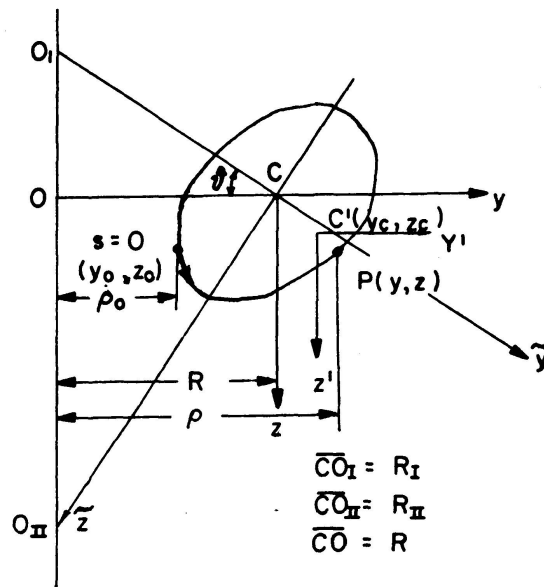


Fig. 1. Systems of coordinate.

A point C is chosen as the origin, and the rectangular coordinate y and z are taken in the radial outward direction and in the vertical downward direction respectively at the cross section. Besides, the curvilinear coordinates s are taken along the middle line of the thin plate member in the cross section. Then, the geometrical moments of area for curved girder may be defined as follows:

$$G_y = R \int_F \frac{z}{n \rho} t ds, \quad (1_1)$$

$$G_z = R \int_F \frac{y}{n \rho} t ds, \quad (1_2)$$

where R represents the radius of curvature of the girder axis formed by connecting the centroid of the cross section, t denotes the thickness of the thin plate member, and n the ratio of the Young's modulus of the steel to that of normal stress-carrying material at a considering point P — for instance, $n = E_s/E_c$ for slab concrete in composite girder where E_s is the Young's modulus of the steel and E_c is that of the concrete —, and ρ the distance between the point P and the center of curvature O as measured in the radial direction of that curved girder.

Next, the point C' having the coordinates (y_c, z_c) is chosen as origin, and the rectangular coordinates (y', z') are taken in parallel with the original ones (y, z) . So, the geometrical moment of area $G_{y'}$, $G_{z'}$ with respect to the new coordinate axes are evaluated by the following formulae:

$$\begin{aligned} G_{y'} &= G_y - z_c F_s, \\ G_{z'} &= G_z - y_c F_s, \end{aligned}$$

where $F_s = R \int_F \frac{t}{n\rho} ds$, the area of the transformed cross section. As described later, if the point C coincides with the centroid, above equation may be written

$$F_s = \int_F \frac{t}{n} ds.$$

When both geometrical moments of area with respect to any pair of mutually perpendicular axes passing through a point O_n are equal to zero, the point O_n is defined as the centroid of the cross section of curved girder.

Let us denote the coordinates of the centroid O_n as (y_n, z_n) , so the situation of the centroid is decided by the following formula:

$$y_n = \frac{G_z}{F_s}, \quad z_n = \frac{G_y}{F_s}. \quad (2)$$

Again, in the thin-walled cross section as shown in Fig. 1, the quantities expressed by the following formulae are defined as the geometrical moment of inertia with respect to the axis y and z respectively,

$$\begin{aligned} I_y &= R \int_F \frac{z^2 t}{n\rho} ds, \\ I_z &= R \int_F \frac{y^2 t}{n\rho} ds. \end{aligned} \quad (3)$$

In the similar manner,

$$I_{yz} = R \int_F \frac{yz t}{n\rho} ds \quad (4)$$

is defined as the product inertia of area.

The sectional moment of the second order $I_{y'}$, $I_{z'}$, with respect to any other rectangular coordinates (y', z') laid in parallel with those (y, z) are evaluated by the following formulae:

$$\begin{aligned} I_{y'} &= I_y - 2z_c G_y + z_c^2 F_s, \\ I_{z'} &= I_z - 2y_c G_z + y_c^2 F_s, \\ I_{y'z'} &= I_{yz} - y_c G_y - z_c G_z + y_c z_c F_s. \end{aligned}$$

In particular case when the origin C coincides with the centroid, since both G_y and G_z are equal to zero,

$$\begin{aligned} I_{y'} &= I_y + z_c^2 F_s, \\ I_{z'} &= I_z + y_c^2 F_s, \\ I_{y'z'} &= I_{yz} + y_c z_c F_s. \end{aligned}$$

If any other coordinate (\tilde{y}, \tilde{z}) have the common origin O with the coordinate (y, z) and incline in the clockwise direction at an angle ϑ , the relations between the sectional moments of the 2nd order with respect to both coordinate axes may be evaluated as follows:

$$\begin{aligned} I_{\tilde{y}} &= I_z \sin^2 \vartheta + I_y \cos^2 \vartheta - I_{yz} \sin 2\vartheta, \\ I_{\tilde{z}} &= I_z \cos^2 \vartheta + I_y \sin^2 \vartheta + I_{yz} \sin 2\vartheta, \\ I_{\tilde{y}\tilde{z}} &= \frac{I_y - I_z}{2} \sin 2\vartheta + I_{yz} \cos 2\vartheta. \end{aligned}$$

Note the invariant relationship

$$\begin{aligned} I_{\tilde{y}} + I_{\tilde{z}} &= I_y + I_z, \\ I_{\tilde{y}} I_{\tilde{z}} - I_{\tilde{y}\tilde{z}}^2 &= I_y I_z - I_{yz}^2. \end{aligned}$$

It can be noted from above formulae that the sectional moments of the 2nd order with respect to the new coordinate axes vary according to the magnitude of the angle of inclination ϑ .

In the special case where the sectional moment of the 2nd order will reach the maximum or minimum value, the coordinate axes will be defined as the principal axes of the cross section, and then the sectional moment of the 2nd order with respect to those axes might be called the principal moment of inertia.

If it is assumed that the sectional moments of the 2nd order I_y , I_z , I_{yz} with respect to arbitrary rectangular axes Oy and Oz have been known, the direction of the principal axis and both maximum and minimum sectional moments of the 2nd order may be easily found. That is to say, by the following condition

$$\frac{dI_{\tilde{y}}}{d\vartheta} = 0,$$

the angle ϑ to specify the direction of the principal axis may be evaluated as follows:

$$\vartheta = \frac{1}{2} \tan^{-1} \frac{2 I_{yz}}{I_z - I_y}.$$

In this special case, it may readily be noted that $I_{\tilde{y}\tilde{z}}$ vanishes, so the simplified relations may be expressed as follows:

$$\begin{aligned} I_{\tilde{y}} I_{\tilde{z}} &= I_y I_z - I_{yz}^2, \\ I_{\tilde{y}} + I_{\tilde{z}} &= I_y + I_z \end{aligned}$$

and then $I_{\tilde{y}}$ and $I_{\tilde{z}}$ will be either the maximum or minimum sectional moment of the 2nd. order respectively. Their values will be given by the following formula:

$$I_{\tilde{y}} \text{ or } I_{\tilde{z}} = \frac{1}{2} \{I_y + I_z \pm \sqrt{(I_y - I_z)^2 + 4 I_{yz}^2}\}.$$

2. System of Coordinates and Stress Resultants at Cross Section

As shown in Fig. 2, the center of curvature O of the girder axis is taken as the origin, and the coordinates ζ are taken perpendicularly upward to the plane including the girder axis, and the coordinates ρ in the radial direction over that plane. Here, the axis $O\rho$ is assumed to pass through the centroid of the cross section.

Next, the cylindrical coordinates φ are taken from the primitive line OA in the peripheral direction along the girder axis toward the other end B of the

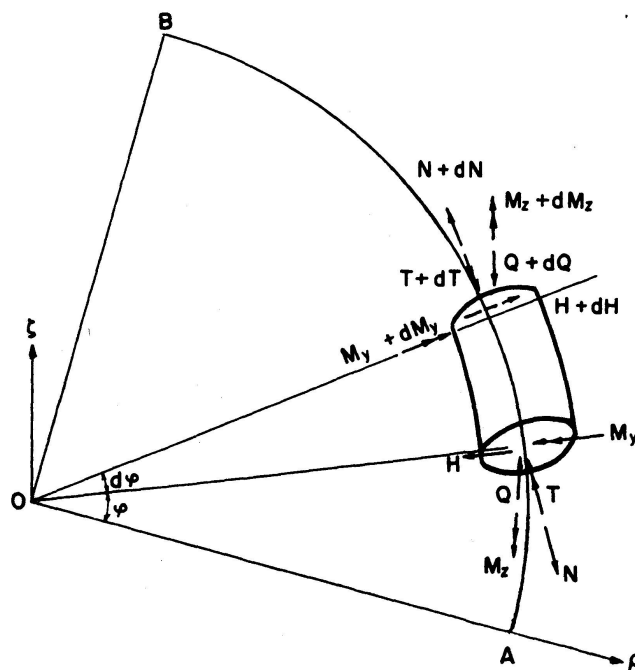


Fig. 2. The system of coordinates and stress resultants produced at any cross-section of a curved girder.

girder. The origin of these cylindrical coordinates (ρ, φ, ζ) is the center of curvature 0. Moreover, let us take a pair of orthogonal axes $0_n y$ and $0_n z$ through the centroid 0_n . An axis $0_n y$ is parallel to and in the same direction as axis 0ρ , and another axis $0_n z$ is parallel to and in the reversal direction as axis 0ζ .

These rectangular coordinates (y, z) are assumed to be fixed to the cross section of girder.

Likewise, another pair of coordinates (\tilde{y}, \tilde{z}) having the common origin 0_n with the coordinates (y, z) are introduced in the direction of the corresponding principal axes of the cross section.

In this case, the axis $0\tilde{y}$ is inclined at an angle ϑ to the axis $0y$ in the clockwise direction.

Now, the stress resultants induced at any cross section of curved are denoted as follows:

1. The shearing forces in the directions of the axis $0_n y$ and $0_n z$ by H and Q , respectively;
2. the axial force acting on the centroid in the direction of the girder axis by N ;
3. the bending moments about the axes $0y$ and $0z$ by M_y and M_z respectively, and
4. the torsional moment about the axis of shear center by T .

3. Pure Torsion

This paragraph deals with the deformations and stresses of curved girder under pure torsion. In this case, end pure torque $T_A = T_0$ and $T_B = T_0$ act on both ends A and B of a free curved girder mutually in the opposite direction as indicated in Fig. 3. It is necessary to act suitable external forces besides this torque for static equilibrium of whole structure unlike the straight girder. In other words, the reactions $V_A = V$ and $V_B = V$ should be applied at both supports A and B . The magnitude of V may be evaluated by

$$V = T_0/R_0, \quad (a)$$

where R_0 is the distance as measured between the shear center and the center of curvature 0. Regarding the shear center further description will be given in paragraph 12. In each Figure, the symbol \leftarrow indicates the necessary torque to advance the right hand screw in the direction of its arrow.

The symbol \odot indicates the force acting in the direction perpendicular to the plane of this paper and toward the back, while the symbol \oplus has a meaning reverse to what was above described. Now, let us consider the stress resultants under pure torsion at any cross section C which is situated at an angle φ' measured from the primitive line $0A$.

From the conditions of static equilibrium of a free body \widehat{AC} cut off by the cross section C , the torsional moment T , the bending moment M_y , and the shearing force Q are expressed as follows:

$$\begin{aligned}
T &= T_0 \cos \varphi' + V R_0 (1 - \cos \varphi'), \\
M_y &= -T_0 \sin \varphi' + V R_0 \sin \varphi', \\
Q &= V.
\end{aligned}$$

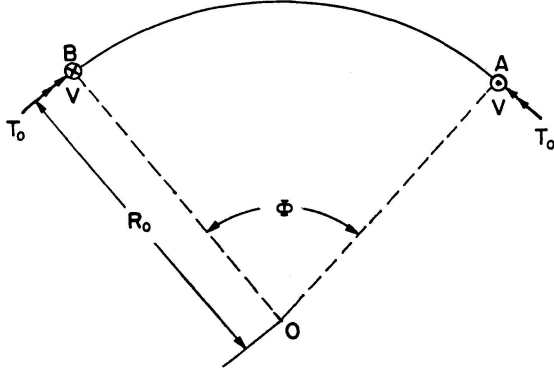


Fig. 3. Pure torsion.

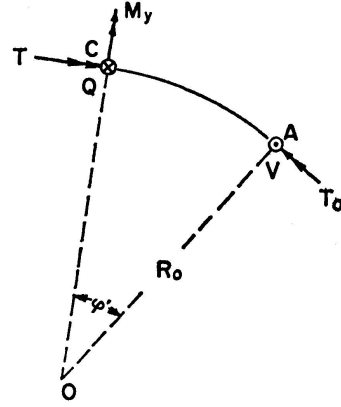


Fig. 4. Stress resultants at any cross section under pure torsion.

Applying above relation (a),

$$T = T_0, \quad M_y = 0.$$

It can be seen that the uniform torsional moment T_0 and uniform shearing force V are produced, but no bending moment is presented.

Generally in cylindrical coordinates, the required relations between six components of the strain and the corresponding three components of the displacement can be written as follows:

$$\begin{aligned}
\epsilon_\rho &= \frac{\partial u}{\partial \rho}, & \epsilon_\varphi &= \frac{1}{\rho} \frac{\partial w}{\partial \varphi} + \frac{u}{\rho}, & \epsilon_\zeta &= \frac{\partial v}{\partial \zeta}, \\
\gamma_{\rho\varphi} &= \frac{1}{\rho} \frac{\partial u}{\partial \varphi} + \frac{\partial w}{\partial \rho} - \frac{w}{\rho}, & \gamma_{\varphi\zeta} &= \frac{\partial w}{\partial \zeta} + \frac{1}{\rho} \frac{\partial v}{\partial \varphi}, & \gamma_{\zeta\rho} &= \frac{\partial v}{\partial \rho} + \frac{\partial u}{\partial \zeta}.
\end{aligned} \tag{5}$$

Furthermore, under pure torsion, the displacements u , v , w at any point $D(\rho, \varphi, \zeta)$ within the girder should be investigated. For that purpose, let us take the shear center S of the cross section as the origin, through which a pair of axes of rectangular coordinates (Y, Z) shall be fixed perpendicularly downward and radially outward at the cross section. Thus, any point at the cross section can be expressed by those coordinates (Y, Z) .

We must take into consideration the differential change $d\theta = d\theta/d\varphi' \cdot d\varphi'$ of the torsional angle θ in the case where the peripheral coordinates φ' change by the differential quantity $d\varphi'$. So, the difference in the displacements of two adjacent points (Y, Z) in the cross section C' situated at the peripheral coordinates $\varphi' + d\varphi'$ and in the cross section C at φ' are $du = Z d\theta$ and $dv = Y d\theta$ in the ρ -direction and the ζ -direction respectively.

How much contribution do these relative displacements of two neigh-

bouring cross sections C , C' make to the displacement of the points (Y, Z) at another cross section D ?

As it may be seen in Fig. 6, the displacements u and w in the plane of girder axis may be expressed by the following formulae:

$$u = \int_0^{\varphi} Z \frac{d\theta}{d\varphi'} \cos(\varphi - \varphi') d\varphi',$$

$$w = - \int_0^{\varphi} Z \frac{d\theta}{d\varphi'} \sin(\varphi - \varphi') d\varphi' + \frac{W_s}{R^2} \rho \frac{d\theta}{d\varphi}. \quad (6)$$

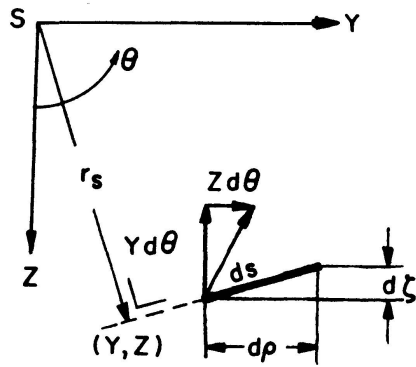


Fig. 5. Differential element ds and rectangular coordinates (Y, Z) .

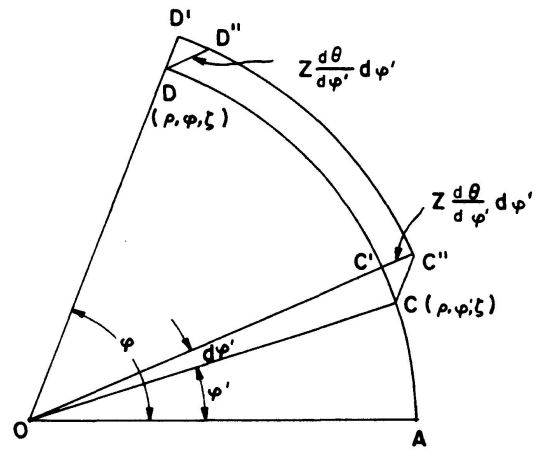


Fig. 6. Displacements u and w under pure torsion.

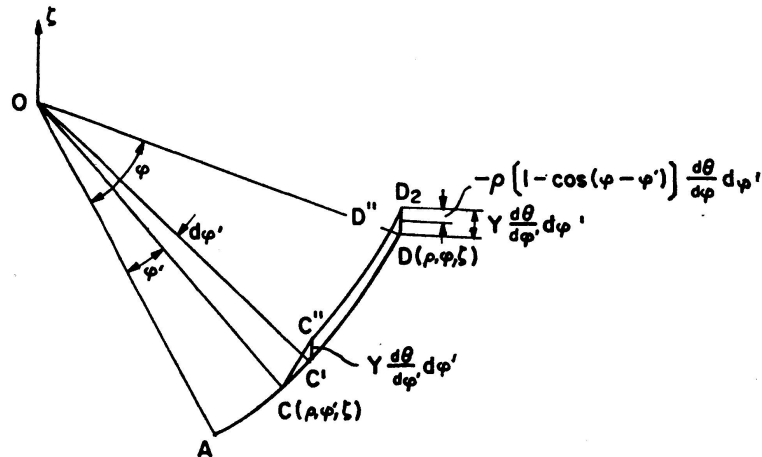


Fig. 7. Displacement v under pure torsion.

On the other hand, the displacement v in the ζ -direction may be expressed by a following formula according to Fig. 7.

$$v = \int_0^{\varphi} \{Y - \rho [1 - \cos(\varphi - \varphi')]\} \frac{d\theta}{d\varphi'} d\varphi'. \quad (7)$$

The second term of the expression (6), represents the warping due to torsion bending phenomena.

Next, by substituting the displacements (6) and (7) into the fundamental Eqs. (5), the strain components may be given as follows:

$$\epsilon_\rho = 0, \quad \epsilon_\zeta = 0, \quad \epsilon_\varphi = W_s \frac{d^2 \theta}{R^2 d\varphi^2}, \quad (8)$$

$$\begin{aligned} \gamma_{\rho\varphi} = & \frac{1}{\rho} \left[- \int_0^\varphi Z \frac{d\theta}{d\varphi'} \sin(\varphi - \varphi') d\varphi' + Z \frac{d\theta}{d\varphi} \right] + \left(\frac{\partial W_s}{\partial \rho} \rho + W_s \right) \frac{d\theta}{R^2 d\varphi} \\ & - \frac{1}{\rho} \left[- \int_0^\varphi Z \frac{d\theta}{d\varphi'} \sin(\varphi - \varphi') d\varphi' + W_s \rho \frac{d\theta}{R^2 d\varphi} \right]. \end{aligned} \quad (9)$$

Assuming that the middle plane of the thin-walled member is inclined at the angle α to the axis 0ρ at the considering point D now, the tangential direction of the curvilinear coordinates s will have come to be inclined at the same angle α to the axis 0ρ . If the coordinate n is introduced in an outward direction perpendicular to the coordinate s as shown in Fig. 8, the following relations may be obtained:

$$\frac{\partial W_s}{\partial \rho} = \frac{\partial W_s}{\partial s} \cos \alpha + \frac{\partial W_s}{\partial n} \sin \alpha, \quad \frac{\partial W_s}{\partial \zeta} = \frac{\partial W_s}{\partial s} \sin \alpha - \frac{\partial W_s}{\partial n} \cos \alpha.$$

Substituting these relations into the Eq. (9),

$$\gamma_{\rho\varphi} = \left(\frac{\partial W_s}{\partial s} \frac{\rho}{R^2} \cos \alpha + \frac{Z}{\rho} + \frac{\partial W_s}{\partial n} \frac{\rho}{R^2} \sin \alpha \right) \frac{d\theta}{d\varphi}. \quad (9')$$

In the same way,

$$\gamma_{\zeta\varphi} = \left(\frac{\partial W_s}{\partial s} \frac{\rho}{R^2} \sin \alpha + \frac{Y}{\rho} - \frac{\partial W_s}{\partial n} \frac{\rho}{R^2} \cos \alpha \right) \frac{d\theta}{d\varphi}, \quad \gamma_{\zeta\rho} = 0. \quad (10)$$

The relationship between the corresponding strain components in the directions of the rectangular coordinates (ρ, ζ, φ) and those in (s, n, φ) can be readily written as follows:

$$\begin{aligned} \epsilon_s &= \epsilon_\rho \cos^2 \alpha + \epsilon_\zeta \sin^2 \alpha + 2\gamma_{\rho\zeta} \cos \alpha \sin \alpha, \\ \gamma_{s\varphi} &= \gamma_{\rho\varphi} \cos \alpha + \gamma_{\zeta\varphi} \sin \alpha, \\ \gamma_{n\varphi} &= \gamma_{\rho\varphi} \sin \alpha - \gamma_{\zeta\varphi} \cos \alpha. \end{aligned} \quad (11)$$

Again substituting the Eqs. (8), (9) and (10) into the Eq. (11), the following simplified formulae can be easily obtained.

$$\epsilon_s = 0, \quad \gamma_{s\varphi} = \left(\frac{\partial W_s}{\partial s} \frac{\rho}{R^2} + \frac{Y}{\rho} \sin \alpha + \frac{Z}{\rho} \cos \alpha \right) \frac{d\theta}{d\varphi}.$$

From the geometrical relationship between the position of the point D and that of the shear center S taken as the center of torsion shown as in Fig. 8,

$Y \sin \alpha + Z \cos \alpha = r_s$ where r_s denote the distance from the tangent DH at D to the shear center. Then the shear strain of angles (s, φ) and (n, φ) will be readily obtained as follows:

$$\gamma_{s\varphi} = \left(\frac{\partial W_s}{\partial s} \frac{\rho}{R^2} + \frac{r_s}{\rho} \right) \frac{d\theta}{d\varphi}, \quad \gamma_{n\varphi} = \left(\frac{\partial W_s}{\partial n} \frac{\rho}{R^2} - \frac{r_n}{\rho} \right) \frac{d\theta}{d\varphi}, \quad (12)$$

where r_n denotes the distance from the normal Dn at D to the shear center.

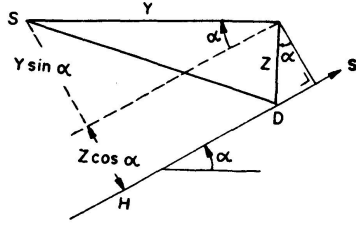


Fig. 8. Relative position of shear center to a differential element.

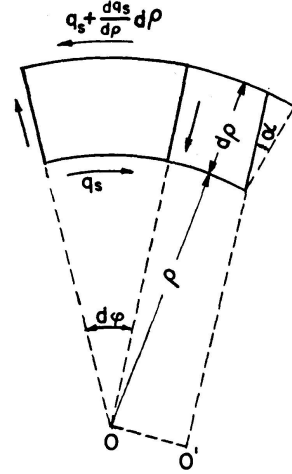


Fig. 9. Stresses under pure torsion.

Accordingly, the stress components may be found as follows:

$$\begin{aligned} \sigma_\varphi &= E_s \frac{W_s}{n} \frac{d^2 \theta}{R^2 d\varphi^2} (= \sigma_w), \\ \tau_{s\varphi} &= G \left(\frac{\partial W_s}{\partial s} \frac{\rho}{R^2} + \frac{r_s}{\rho} \right) \frac{d\theta}{d\varphi}, \\ \tau_{n\varphi} &= G \left(\frac{\partial W_s}{\partial n} \frac{\rho}{R^2} - \frac{r_n}{\rho} \right) \frac{d\theta}{d\varphi}. \end{aligned} \quad (13)$$

In the case of pure torsion, no normal stress σ_φ is produced because $d\theta/d\varphi$ become constant, and the shearing stress $\tau_{n\varphi}$ is generally small.

Next, let us consider the static equilibrium concerning the differential elements cut out from the girder by two neighbouring cylindrical sections with radii ρ and $\rho + d\rho$ and two radial sections interacting on each other at a differential angle $d\varphi$. As already described, there are only shearing stresses $\tau_{s\varphi}$ which are uniformly distributed over the thickness t and are parallel to the tangent to the middle plane of the thin member. So, the shear flow q_s along the cylindrical section with a radius ρ is expressed by the definition.

$$q_s = \tau_{s\varphi} t. \quad (14)$$

About the differential element as shown in Fig. 9, let us consider the equilibrium of two shear flows in the peripheral direction.

Here the middle plane of the element is assumed to be inclined at any angle α to the axis $O\rho$. Then the equilibrium condition of the moments about

the point O' , where the axis $O\zeta$ intersects with the plane including the element, may be expressed as follows:

$$q_s \rho^2 d\varphi \sec \alpha = \left(q_s + \frac{dq_s}{d\rho} d\rho \right) (\rho + d\rho)^2 d\varphi \sec \alpha.$$

Neglecting the second order of the differential term,

$$\frac{dq_s}{d\rho} \rho^2 + 2 q_s \rho = 0.$$

Solving this differential equation, the following general solution can be obtained,

$$q_s \rho^2 = \text{const.}$$

It may thus be noted that the magnitude of the shear flow q_s is inversely proportional to the square of the coordinates ρ of the considering point.

Now, let us the shear flow going around the k th. cell denote q_{sk} , and then put the integral constant equal to $R^2 q_k$ for the k th. cell. Then the following equation will be obtained,

$$q_{s,k} \rho^2 = R^2 q_k.$$

Consequently, at the point ρ belonging to the k th. cell, the shear flow q_{sk} will have the following magnitude,

$$q_{s,k} = \frac{R^2}{\rho^2} q_k. \quad (15)$$

In the Eq. (15), q_k will be called the standard shear flow belonging to the k th. cell.

The Eq. (15) always be satisfied for the closed cross section with arbitrary shape. If the girder has any closed section with multiple cells, the shear flow q_s in the thin member surrounding the k th. cell may generally be given as follows:

$$q_s = q_{s,k} \quad \text{In the nonboundary wall belonging to the } k \text{th. cell,} \quad (16_1)$$

$$q_s = q_{s,k} - q_{s,k-1} \quad \text{in the boundary wall between the } k \text{th. and } (k-1) \text{th. cell,} \quad (16_2)$$

$$q_s = q_{s,k} - q_{s,k+1} \quad \text{in the boundary wall between the } k \text{th. and } (k+1) \text{th. cell.} \quad (16_3)$$

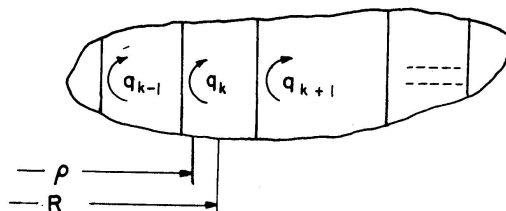


Fig. 10. Section with multiple cells.

Furthermore, the torsional function \tilde{q}_k is defined by

$$q_k = G_s \frac{d\theta}{R d\varphi} \tilde{q}_k, \quad (17)$$

where G_s is the shear modulus of elasticity of steel. Substituting the Eq. (15) into the Eq. (17), the circulating shear flow $q_{s,k}$ is easily obtained.

$$q_{s,k} = \left(\frac{R}{\rho}\right)^2 G_s \frac{d\theta}{R d\varphi} \tilde{q}_k. \quad (17')$$

Hence, by applying the Eq. (17') to the Eq. (16), the shear flow q_s in the wall belonging to the k th. cell will have the following value:

$$\begin{aligned} q_s &= \left(\frac{R^2}{\rho^2} \tilde{q}_k - \frac{R^2}{\rho^2} \tilde{q}_{k\pm 1}\right) G_s \frac{d\theta}{R d\varphi} && \text{in the boundary wall,} \\ q_s &= \frac{R^2}{\rho^2} \tilde{q}_k G_s \frac{d\theta}{R d\varphi} && \text{in the nonboundary wall.} \end{aligned} \quad (18)$$

By applying above result to the Eq. (13₂), and then integrating it with respect to s ,

$$W_s = \bar{W}_s + W_0, \quad (19)$$

where W_0 represents the value of W_s at the original point $s=0$.

Besides, \bar{W}_s may be evaluated as follows:

$$\begin{aligned} \bar{W}_s &= \int_0^s \frac{R^3}{\rho^3} \tilde{q}_k \frac{n_g}{t} ds - \int_0^s \frac{R^3}{\rho^3} \tilde{q}_{k\pm 1} \frac{n_g}{t} ds - R^2 \int_0^s \frac{r_s}{\rho^2} ds && \text{in the boundary wall,} \\ \bar{W}_s &= \int_0^s \frac{R^3}{\rho^3} \tilde{q}_k \frac{n_g}{t} ds - R^2 \int_0^s \frac{r_s}{\rho^2} ds && \text{in the nonboundary wall.} \end{aligned} \quad (20)$$

Now, let us take the curvilinear integral around the k th. cell, then the following equation may be obtained by means of the periodicity of W_s value.

$$\oint_k \frac{\partial W_s}{\partial s} ds = 0. \quad (21)$$

By applying the conditions (21) to each cell, the following simultaneous equations for \tilde{q}_k can be readily obtained.

$$-\tilde{q}_{k-1} \int_{k-1,k} \frac{R^3}{\rho^3} \frac{n_g}{t} ds + \tilde{q}_k \oint_k \frac{R^3}{\rho^3} \frac{n_g}{t} ds - \tilde{q}_{k+1} \int_{k,k+1} \frac{R^3}{\rho^3} \frac{n_g}{t} ds = R^2 \oint_k \frac{r_s}{\rho^2} ds. \quad (22)$$

Where \oint_k is curvilinear integral around the k th. cell, and $\int_{k,k\pm 1}$ boundary wall between the k th. and the $k \pm 1$ th. cell.

The expression for torsional moment becomes

$$T_s = \int_F q_s r_s ds.$$

Substituting the Eq. (17') into above expression, we obtain

$$T_s = G_s J \frac{d\theta}{R d\varphi}, \quad (23)$$

where $G_s J$ denotes the torsional rigidity and the torsion constant J can be evaluated as follows:

$$J = \sum_F \tilde{q}_k R^2 \oint_k \frac{r_s}{\rho^2} ds, \quad (24)$$

where \sum_F indicates the summation all over the cross section.

In the Eq. (23), since T_s is constant, $d\theta/d\varphi$ is also constant for the girder with the uniform section. Then, by eliminating θ from both Eq. (17) and (23), the shear flow q_{sk} can be given as the function of the torsional moment T_s .

$$q_{s,k} = \frac{R^2}{\rho^2} \frac{T_s}{J} \tilde{q}_k. \quad (25)$$

4. Pure Bending Normal to the Plane of Curvature

Pure bending normal to the plane of curvature before deformation is defined as the condition of deformation in the case where the curved girder is bent so as to deflect along the side surface of a cone the vertex of which coincides with the center of curvature 0. In this fundamental deformation, the differential element $CC'BB'$ which is initially situated in the plane of the sector OAD and cut out by the diametric radii OC and OC' holding the differential angle $d\varphi'$, will remain on the common plane $0CC''$ even after deforming. Then the section $B'C'$ has come to be inclined at angle $d\gamma$ to the section BC and translate to $B''C''$. That is to say, $\angle B'BB'' = \angle C'CC'' = d\gamma$, and that $d\gamma/d\varphi'$ is constant all over the girder.

By the relative inclination between the two adjacent sections, the displacement components of the point $D(\rho, \varphi, \zeta)$ at the section φ will be consequently found by the following formulae,

$$\begin{aligned} u &= \int_0^\varphi \sin(\varphi - \varphi') z \frac{d\gamma}{d\varphi'} d\varphi', & v &= \int_0^\varphi \rho \sin(\varphi - \varphi') \frac{d\gamma}{d\varphi'} d\varphi', \\ w &= \int_0^\varphi \cos(\varphi - \varphi') z \frac{d\gamma}{d\varphi'} d\varphi', \end{aligned} \quad (26)$$

where z is the distance between the point D and the neutral axis of the girder section.

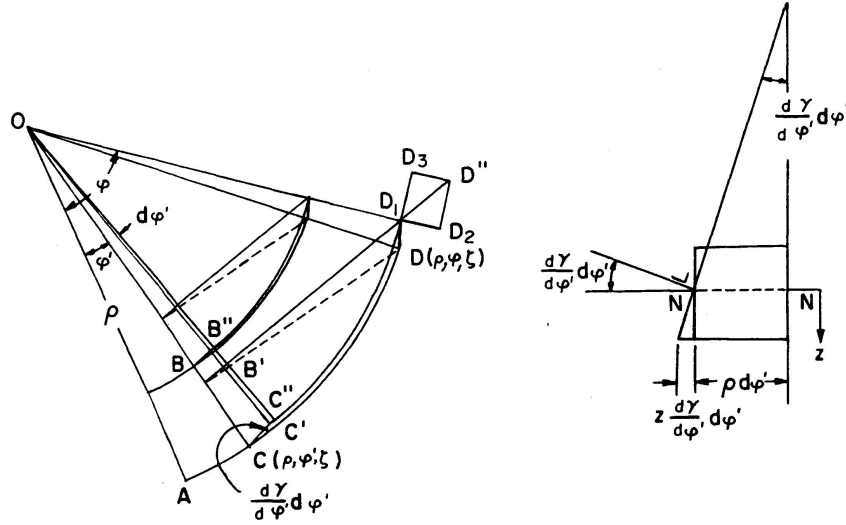


Fig. 11. Displacements under pure bending normal to the plane of curvature.

By substituting the Eq. (26) into the fundamental equation of the strain components (5),

$$\epsilon_\rho = \epsilon_\zeta = \gamma_{\rho\varphi} = \gamma_{\varphi\zeta} = \gamma_{\zeta\rho} = 0, \quad \epsilon_\varphi = \frac{z}{\rho} \frac{d\gamma}{d\varphi}.$$

Thereafter, only stress components are induced

$$\sigma_\varphi = E_s \frac{z}{n\rho} \frac{d\gamma}{d\varphi} \quad (27)$$

and all others are nothing.

5. Pure Bending in the Plane of Curvature

Let us define as pure bending in the initial curvature the condition of deformation in the case where the girder is bent so as to be wound into the cylindrical surface the axis of which is 0ζ , namely, the perpendicular through the center of curvature 0 .

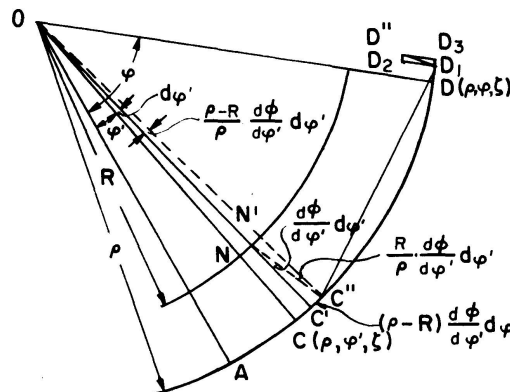


Fig. 12. Pure bending in its own plane.

In the plane of the initial curvature, the adjacent section $N'C'$ defined by angle $\varphi' + d\varphi'$ rotates at differential angle $d\phi'$ relatively to the section NC defined by angle φ' , after deforming as shown in Fig. 12.

Due to this deformation, the displacement u, v, w of the point D at the section φ will be given as follows:

$$u = -\int_0^\varphi R \sin(\varphi - \varphi') \frac{d\phi}{d\varphi'} d\varphi', \quad v = 0, \quad w = \int_0^\varphi [\rho - R \cos(\varphi - \varphi')] \frac{d\phi}{d\varphi'} d\varphi'. \quad (28)$$

If these values are substituted into the fundamental equations of the strain components (5),

$$\epsilon_\rho = \epsilon_\zeta = \gamma_{\rho\varphi} = \gamma_{\varphi\zeta} = \gamma_{\zeta\rho} = 0, \quad \epsilon_\varphi = \frac{y}{\rho} \frac{d\phi}{d\varphi},$$

hence the stress components will be expressed as follows:

$$\sigma_\varphi = \frac{E_s}{n} \frac{y}{\rho} \frac{d\phi}{d\varphi}. \quad (29)$$

6. Pure Bending About the Principal Axis $0_n \tilde{y}$

Let us act two equal end moments M_I about the principal axis of the cross section and at the same time the uniformly distributed torque M_I/R_I per unit length along the girder axis in order to maintain the statical equilibrium as shown in Fig. 13.

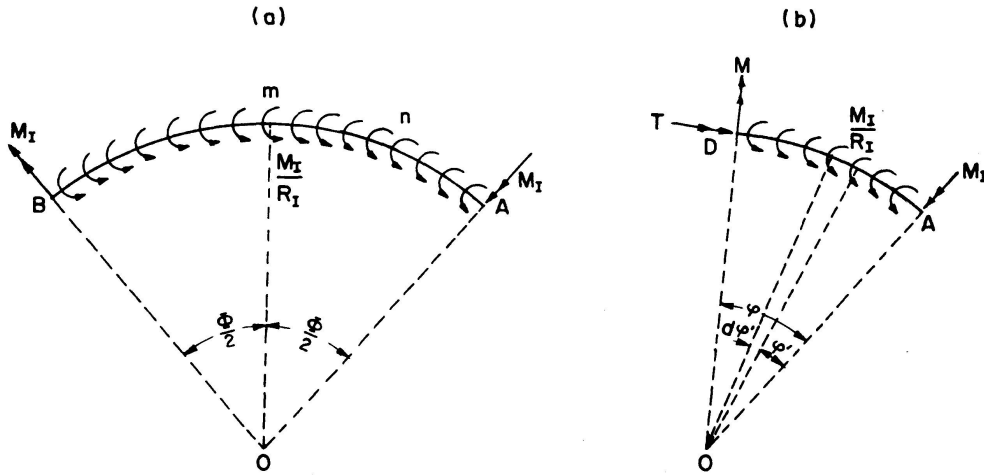


Fig. 13. External and internal forces under pure bending about the principal axis $0_n \tilde{y}$.

The stress resultants at any section D are calculated as follows:

$$Q = 0,$$

$$\tilde{M}_{\tilde{y}} = \left\{ M_I \cos \varphi + \int_0^\varphi \frac{M_I}{R} \sin(\varphi - \varphi') R d\varphi' \right\} \cos^2 \vartheta + M_I \sin^2 \vartheta = M_I,$$

$$T = \{ M_I \sin \varphi - \int_0^\varphi M_I \cos(\varphi - \varphi') d\varphi' \} \cos \vartheta = 0.$$

It may be noted from the above equations that the constant moment M_I about the principal axis $0_n \tilde{y}$ is produced all over the girder axis, and no other

stress resultants are present everywhere. This is nothing but a state of pure bending.

If the girder has a uniform section, it also has a condition of uniform deformation, namely, the constant curvature $d\eta/d\varphi'$. Thus, the displacements at the point $D(\rho, \varphi, \zeta)$ will be found from expressions (26) and (28) as follows:

$$\begin{aligned} u &= \int_0^\varphi \left\{ \sin(\varphi - \varphi') z \frac{d\eta}{d\varphi'} \cos \vartheta + R \sin(\varphi - \varphi') \frac{d\eta}{d\varphi'} \sin \vartheta \right\} d\varphi', \\ v &= \int_0^\varphi \rho \sin(\varphi - \varphi') \frac{d\eta}{d\varphi'} \cos \vartheta d\varphi', \\ w &= \int_0^\varphi \left\{ \cos(\varphi - \varphi') z \frac{d\eta}{d\varphi'} \cos \vartheta + [R \cos(\varphi - \varphi') - \rho] \frac{d\eta}{d\varphi'} \sin \vartheta \right\} d\varphi'. \end{aligned}$$

Substituting the above expressions in the fundamental equation of strain components (5).

$$\epsilon_\rho = \epsilon_\zeta = \gamma_{\rho\varphi} = \gamma_{\varphi\zeta} = \gamma_{\zeta\rho} = 0, \quad \epsilon_\varphi = \frac{\tilde{z}}{\rho} \frac{d\eta}{d\varphi}.$$

Hence, the only stress components are produced as follows:

$$\sigma_\varphi = E_s \frac{\tilde{z}}{n\rho} \frac{d\eta}{d\varphi} (= \sigma_I) \quad (a)$$

and all others are nothing.

The relation between the bending moment $M_{\tilde{y}}$ and the normal stress σ_I may be obtained as follows:

$$M_{\tilde{y}} = \int_F \sigma_I \tilde{z} dF.$$

By substituting the Eq. (a) in the above equation,

$$M_{\tilde{y}} = E_s I_{\tilde{y}} \frac{d\eta}{R d\varphi}, \quad (b)$$

where $I_{\tilde{y}} = \int_F \frac{R\tilde{z}^2}{n\rho} t ds$ is the principal moment of inertia about the principal axis $0_n \tilde{y}$.

Next, by eliminating η from the Eqs. (a) and (b),

$$\sigma_I = \frac{M_{\tilde{y}} \tilde{z}}{n I_{\tilde{y}} \rho} R. \quad (30)$$

As no axial force is presented, the following equation may be given,

$$\int_F \frac{\tilde{z} t}{n\rho} ds = 0. \quad (31)$$

7. Pure Bending About Principal Axis of Section $0_n \tilde{z}$

In the similar way to the pure bending described in the preceding section 6, let us act two end equal moments M_{II} as well as the uniformly distributed torque M_{II}/R_{II} per unit length all over the girder axis.

In this case the stress resultants at any section D are as follows:

$$Q = 0, \quad M_{\tilde{z}} = M_{II}, \quad T = 0.$$

Again, bending moment M_{II} about the principal axis $0_n \tilde{z}$ is produced all over the girder axis, and there are no other stress resultants. This is also a kind of pure bending.

The displacements will be induced at any point D due to constant curvature $d\chi/d\varphi$ after deforming, and may be expressed analogous to Eqs. (26) and (28) as follows:

$$\begin{aligned} u &= \int_0^\varphi \sin(\varphi - \varphi') \frac{d\chi}{d\varphi'} (z \sin \vartheta - R \cos \vartheta) d\varphi', \\ v &= \int_0^\varphi \rho \sin(\varphi - \varphi') \frac{d\chi}{d\varphi'} \sin \vartheta d\varphi', \\ w &= \int_0^\varphi \{[\rho - R \cos(\varphi - \varphi')] \cos \vartheta + \cos(\varphi - \varphi') z \sin \vartheta\} \frac{d\chi}{d\varphi'} d\varphi'. \end{aligned}$$

Substituting the above equations in the equation of strain components (5) again,

$$\epsilon_\rho = \epsilon_\zeta = \gamma_{\rho\varphi} = \gamma_{\varphi\zeta} = \gamma_{\zeta\rho} = 0, \quad \epsilon_\varphi = \frac{\tilde{y}}{\rho} \frac{d\chi}{d\varphi}.$$

Hence, the stress component is only

$$\sigma_\varphi = \frac{E_s}{n} \frac{\tilde{y}}{\rho} \frac{d\chi}{d\varphi} (= \sigma_{II}) \quad (a)$$

and all others are equal to zero.

From the condition of no existence of axial force,

$$\int_F \frac{\tilde{y} t}{n \rho} ds = 0. \quad (32)$$

The bending moment $M_{\tilde{z}}$ is clearly

$$M_{\tilde{z}} = \int_F \sigma_{II} \tilde{y} dF.$$

By substituting the Eq. (a) in the above equation,

$$M_{\tilde{z}} = E_s I_{\tilde{z}} \frac{d\chi}{R d\varphi}, \quad (b)$$

where

$$I_{\tilde{z}} = \int_F \frac{R \tilde{y}^2}{n \rho} t ds. \quad (33)$$

Eliminating φ from the Eqs. (a) and (b),

$$\sigma_{II} = \frac{M_z \tilde{y}}{n I_z} \frac{R}{\rho}.$$

On the other hand, by applying the Eq. (1) to both conditions (31) and (32), and by replacing the coordinates,

$$G_y = 0, \quad G_z = 0. \quad (34)$$

The above equations are nothing but the conditions for determining the position of the neutral axis. From the Eq. (34₂) with attention to $y = \rho - R$,

$$R = \frac{F_s}{\int_F \frac{t}{n \rho} ds}. \quad (35)$$

For the reason that the Eqs. (34) agree with the definition of centroid described in paragraph 1, it may be noted that both neutral axes pass through the centroid O_n .

8. Pure Tension

Let us consider the case where two equal tensile forces N_0 are applied at both ends A and B of a free curved girder as shown in Fig. 14.

In this case, so as to maintain static equilibrium, uniformly distributed radial transverse load N_0 per unit central angle must be applied too.

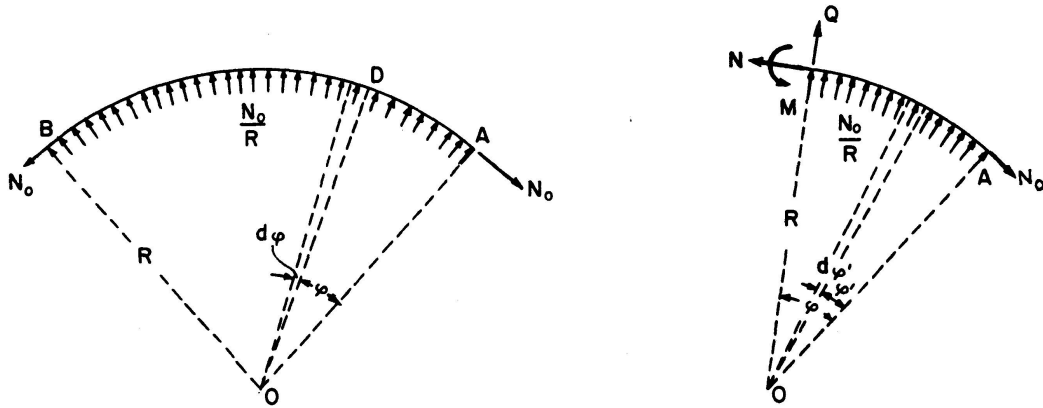


Fig. 14. Pure tension.

Under this loading condition, the stress resultants at the section defined by angle φ may be evaluated as follows:

$$Q = N_0 \sin \varphi - N_0 \int_0^\varphi \cos(\varphi - \varphi') d\varphi' = 0,$$

$$N = N_0 \cos \varphi + N_0 \int_0^\varphi \sin(\varphi - \varphi') d\varphi' = N_0,$$

$$M_z = N_0 R - N R = 0.$$

Consequently, the constant axial force N_0 only is produced.

As shown in Fig. 15, the relative displacement of the adjacent section $N'C'$ defined by angle $\varphi' + d\varphi'$ will be caused to the section NC defined by angle φ , and $N'C'$ will move to $N''C''$.

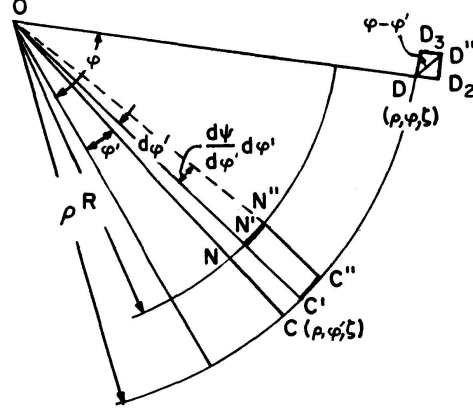


Fig. 15. Displacements under pure tension.

The displacement of the differential fibers NN' and CC' are as follows:

$$N'N'' = C'C'' = R d\psi.$$

Therefore, three displacement components u, v, w at any point $D(\rho, \varphi, \zeta)$ are expressed as follows:

$$u = \int_0^{\varphi} R \frac{d\psi}{d\varphi'} \sin(\varphi - \varphi') d\varphi', \quad v = 0, \quad w = \int_0^{\varphi} R \frac{d\psi}{d\varphi'} \cos(\varphi - \varphi') d\varphi'. \quad (36)$$

The strain components can be readily obtained by substituting the above equation in the Eq. (5).

$$\epsilon_\rho = \epsilon_\zeta = \gamma_{\rho\varphi} = \gamma_{\varphi\zeta} = \gamma_{\zeta\rho} = 0, \quad \epsilon_\varphi = \frac{R}{\rho} \frac{d\psi}{d\varphi}.$$

Therefore, the stress components are

$$\sigma_\varphi = E_s \frac{R}{n\rho} \frac{d\psi}{d\varphi} (= \sigma_n) \quad (a)$$

and all other stress components are vanishing.

The relation between the stress σ_n and the axial force N is expressed as follows:

$$N = \int_F \sigma_n dF.$$

Substituting the Eq. (a) in the above equation

$$N = E_s \frac{d\psi}{d\varphi} \int_F \frac{R}{\rho} \frac{t}{n} ds.$$

By using the Eq. (35),

$$N = E_s F_s \frac{d\psi}{d\varphi}. \quad (b)$$

By eliminating $d\psi/d\varphi$ from both Eq. (a) and (b),

$$\sigma_n = \frac{R}{n\rho} \frac{N}{F_s}. \quad (37)$$

On the other hand, the bending moment M_z about the principal axis $0_n \tilde{z}$ will be found as follows:

$$M_{\tilde{z}} = \int_F \sigma_n \tilde{y} dF.$$

Substituting the Eq. (37) in the above equation, it will be noted that $M_{\tilde{z}}$ vanishes by means of the condition (32). Regarding the bending moment $M_{\tilde{y}}$ about another principal axis $0_n \tilde{y}$ likewise vanishes. That is to say, no bending moment is produced in pure tension.

9. Torsion Bending

If the nonuniformly distributed torque and transverse load are applied at a curved girder so as to maintain the static equilibrium, both the torsional moment T and the shearing force Q produced in the girder vary as the function of variable φ . Such a condition of deformation is defined as torsion bending, and that can be created practically. Since T is here not constant along the girder axis, it can be seen from the Eq. (23) that the specific angle of twist $d\theta/d\varphi$ will also vary along the length of the girder even in the case of uniform section. In the similar manner as the straight girder, the normal stress σ_w is

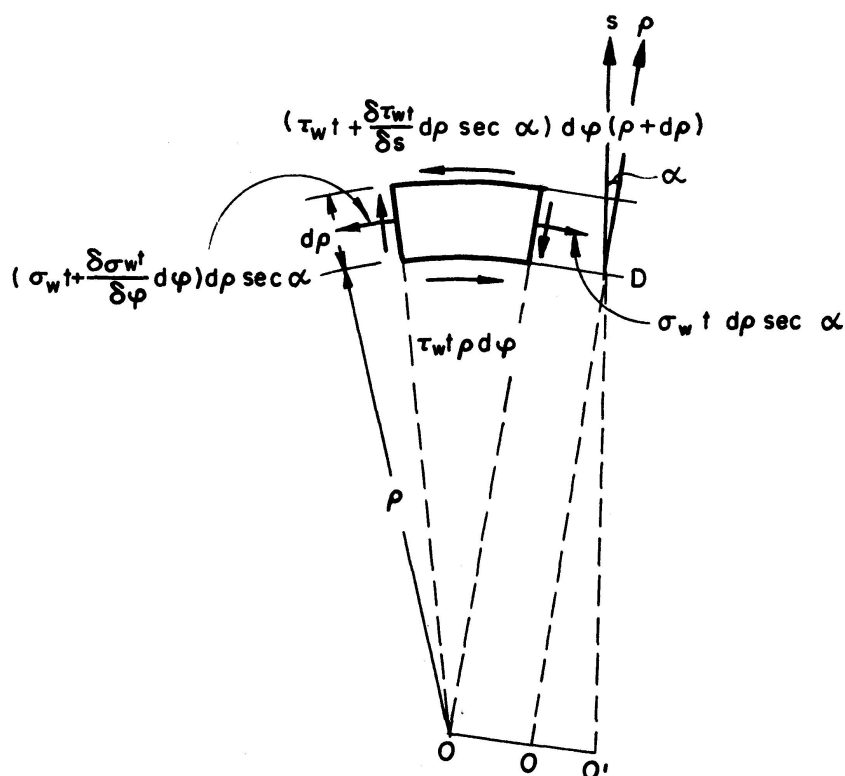


Fig. 16. Stresses under torsion bending.

produced as the result of restraint on warping and its value is found by means of Eq. (13₁). Then the secondary shearing stress τ_w should be induced to resist secondary normal stress σ_w . In order to find this value, let us consider the static equilibrium between the stresses acting on the differential element as shown in Fig. 16. Taking such fact into account that the direction of the middle plane of the differential element is generally inclined at an angle α to that of the axis $O\rho$, the following equation for static equilibrium can be obtained.

$$\frac{\partial \tau_w t}{\partial s} + \frac{2 \tau_w t}{\rho} \cos \alpha + \frac{1}{\rho} \frac{\partial \sigma_w t}{\partial \varphi} = 0. \quad (c)$$

So, let us adopt the following formula as the secondary shear flow q_w .

$$q_w = \tau_w t = -\frac{E_s}{R^3} \frac{d^3 \theta}{d\varphi^3} q^*(s), \quad (38)$$

where q^* is a function of coordinate s only, and will be named as the torsion bending function.

Substituting the Eq. (38) in the differential Eq. (c), and eliminating the common terms,

$$\frac{dq^*}{ds} + 2 \frac{\cos \alpha}{\rho} q^* = \frac{R}{\rho} \frac{W_s t}{n}.$$

By solving this differential equation,

$$q^* = \frac{1}{\rho^2} \left(R \int_0^s W_s \frac{t}{n} \rho ds + S_w \right), \quad (39)$$

where S_w represents the quantity respected to a statically indeterminate shear flow and may be found by the following process.

In the differential element of curved girder included between two radii with the angle $d\varphi$ between them, the potential energy $d\Pi$ will be stored as follows:

$$d\Pi = \frac{1}{2} \int_F \left(\frac{\sigma_w^2}{E} + \frac{\tau^2}{G} \right) t \rho ds d\varphi - T \frac{d\theta}{d\varphi} d\varphi.$$

Therefore, the total potential energy Π of the curved girder is

$$\Pi = \frac{1}{2} \left\{ \int_0^\Phi \int_F \left(\frac{\sigma_w^2}{E} + \frac{\tau^2}{G} \right) t \rho ds d\varphi - \int_0^\Phi T \frac{d\theta}{d\varphi} d\varphi \right\}. \quad (d)$$

Generally, the shearing stress τ_k in the circumferencial wall of the k th. cell is caused partially by shear flow q_{sk} due to pure torsion as discussed in paragraph 3, and partially by the secondary shear flow q_{wk} . In the wall belonging to open cross section, q_s is not present of course.

$$\begin{aligned}
\tau_k &= \frac{1}{t} (q_{sk} + q_{wk}) && \text{Nonboundary wall,} \\
&= \frac{1}{t} (q_{sk} - q_{s,k\pm 1} + q_{wh}) && \text{Boundary wall.}
\end{aligned} \tag{40}$$

Of above expression, q_{wk} may be written in the following form from the Eqs. (38) and (39).

$$\begin{aligned}
q_{wk} &= -\frac{E_s}{R^3} \frac{d^3 \theta}{d\varphi^3} \frac{1}{\rho^2} (\bar{q}_{wk}^* + S_{wh}) && \text{Nonboundary wall,} \\
&= -\frac{E_s}{R^3} \frac{d^3 \theta}{d\varphi^3} \frac{1}{\rho^2} (\bar{q}_{wk}^* + S_{wk} - S_{w,k\pm 1}) && \text{Boundary wall,}
\end{aligned} \tag{41}$$

$$\text{where} \quad \bar{q}_{wk}^* = R \int_0^s W_s \frac{t \rho}{n} ds. \tag{42}$$

By means of the principle of least work, the variation $\delta \Pi$ of Π for the variation δS_{wk} of S_{wk} should be put equal to zero.

$$\delta \Pi = 0.$$

Based on this condition, by the use of the Eqs. (d), and (40) to (42).

$$\begin{aligned}
& -\tilde{q}_{k-1} \frac{d\theta}{R d\varphi} \int_{k,k-1} \frac{R^3 n_g}{\rho^3 t} ds + \tilde{q}_k \frac{d\theta}{R d\varphi} \oint_k \frac{R^3 n_g}{\rho^3 t} ds \\
& -\tilde{q}_{k+1} \frac{d\theta}{R d\varphi} \int_{k,k+1} \frac{R^3 n_g}{\rho^3 t} ds + \oint_k \frac{R q_{wk}}{G \rho t} ds - \frac{d\theta}{R d\varphi} \oint_k \frac{R^2 r_s}{\rho^2} ds = 0.
\end{aligned}$$

The first three terms and the fifth one of the above equation can be eliminated by using the Eq. (22), and then the following equation can be consequently obtained.

$$\oint_k \frac{q_{wk} n_g}{\rho t} ds = 0. \tag{43}$$

Substituting the Eq. (41) in the conditions (43), the simultaneous equations for S_{wk} are obtained.

$$-S_{w,k-1} \int_{k,k-1} \frac{R^3 n_g}{\rho^3 t} ds + S_{wk} \oint_k \frac{R^3 n_g}{\rho^3 t} ds - S_{w,k+1} \int_{k,k+1} \frac{R^3 n_g}{\rho^3 t} ds = -\oint_k \frac{R^3 \bar{q}_{wk}^* n_g}{\rho^3 t} ds. \tag{44}$$

The following integration will be referred to as the warping moment.

$$M_w = \frac{1}{R} \int_F \sigma_w W_s \rho dF. \tag{45}$$

Substituting the stress (13) in Eq. (45), the warping constant C_w can be readily obtained as follows:

$$C_w = \int_F \frac{\rho}{R} W_s^2 \frac{t}{n} ds. \quad (46)$$

Hence, the warping moment M_w may be expressed in the simplified form,

$$M_w = E_s C_w \frac{d^2 \theta}{R^2 d\varphi^2}. \quad (47)$$

From both Eq. (47) and (13₁), the practical formula for the normal stress σ_w due to torsion bending can be obtained in the analogous form to the bending.

$$\sigma_w = \frac{M_w}{C_w} \frac{W_s}{n}. \quad (48)$$

On the other hand, the torsional moment T_w will be produced due to the secondary shear flow q_w .

$$T_w = \int_F q_w r_s ds.$$

Substituting the Eqs. (41) and (42) into above equation, and considering the condition (43), q_w may be transformed as follows:

$$T_w = -E_s C_w \frac{d^3 \theta}{R^3 d\varphi^3}. \quad (49)$$

Finally, since the total torsional moment T can be found as the sum of the two kinds of torsional moment T_s and T_w , from the Eqs. (23) and (49),

$$T = G_s J \frac{d\theta}{R d\varphi} - E_s C_w \frac{d^3 \theta}{R^3 d\varphi^3}. \quad (50)$$

10. General Bending

In this paragraph, let us discuss the general bending, where two mutually perpendicular bending moments M_y , M_z , two corresponding shearing forces H , \bar{Q} , to above moments and an axial force N are simultaneously presented.

In order to clarify the static characteristics in this case, the rectangular coordinates (y, z) as shown in Fig. 17.

The origin is taken to coincide with the centroid O_n of the cross section.

The displacements at any point (y, z) of cross section due to deformation may be found by superimposing the respective displacements given in paragraphs 4, 5, and 8. Therefore, the normal stress σ_x in the general bending may be readily expressed as follows:

$$\sigma_x = a \frac{R}{n \rho} + b \frac{y}{n \rho} + c \frac{z}{n \rho}, \quad (a)$$

where a , b , and c are constant and may be determined from the equilibrium of the stress resultants and stresses,

$$\int_F \sigma_x t ds = N, \quad \int_F \sigma_x z t ds = M_y, \quad \int_F \sigma_x y t ds = M_z.$$

By substituting the Eq. (a) in the above equation, and solving for a , b , and c .

$$\sigma_x = \frac{N}{F_s} \frac{R}{n\rho} + \frac{M_z I_y - M_y I_{yz}}{I_y I_z - I_{yz}^2} \frac{R}{n\rho} y + \frac{M_y I_z - M_z I_{yz}}{I_y I_z - I_{yz}^2} \frac{R}{n\rho} z. \quad (51)$$

Generally, if the stress resultants M_y , M_z and N vary along the girder length, the shearing stress τ should be induced to balance with the normal stress σ_x . Regarding the static equilibrium between σ_x and τ , we arrive the similar equation as the Eq. (c) in paragraph 9.

$$\frac{\partial \tau t}{\partial s} + \frac{2\tau t}{\rho} \cos \alpha + \frac{1}{\rho} \frac{\partial \sigma_x t}{\partial \varphi} = 0. \quad (b)$$

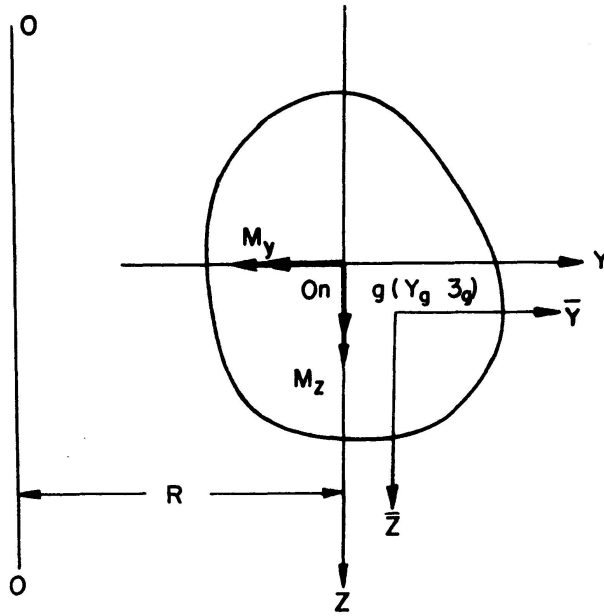


Fig. 17. Rectangular coordinates.

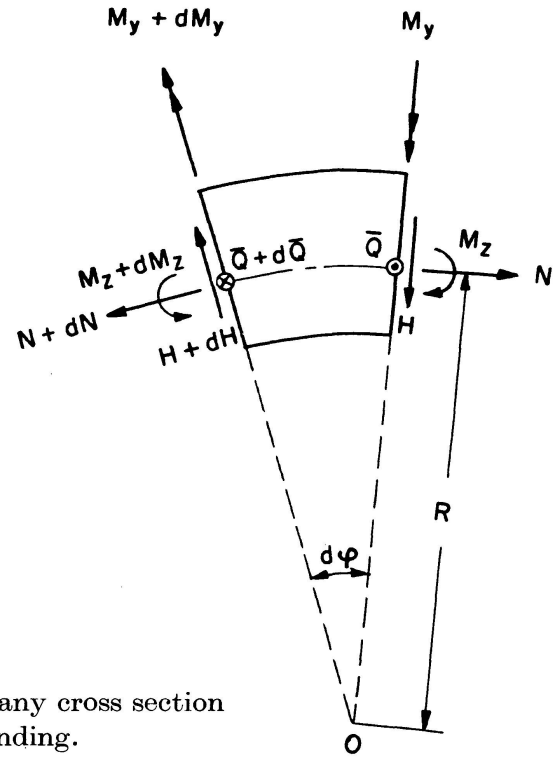


Fig. 18. Internal forces at any cross section under general bending.

From the static equilibrium of the differential elements, the following three equations may be obtained,

$$\frac{dM_z}{d\varphi} = R H, \quad \frac{dN}{d\varphi} = -H, \quad \frac{dM_y}{d\varphi} = R_0 \bar{Q} - H z_s, \quad (52)$$

where \bar{Q} represents the shearing force due to bending about the axis $0_n y$, and z_s is the vertical distance between the shear center and the centroid.

Substituting the Eq. (51) in the Eq. (b), the shear flow q may be expressed under consideration of the relation (52) as follows:

$$q = \tau t = -\{H \check{q}_h(s) + \bar{Q} \check{q}_b(s)\}, \quad (53)$$

where $\check{q}_h(s) = \frac{R}{\rho^2} (\bar{q}_h + S_{h,k})$ Nonboundary wall,

$= \frac{R}{\rho^2} (\bar{q}_h + S_{h,k} - S_{h,k\pm 1})$ Boundary wall,

$$(54)$$

$\check{q}_b(s) = \frac{R_0}{\rho^2} (\bar{q}_b + S_{b,k})$ Nonboundary wall,

$= \frac{R_0}{\rho^2} (\bar{q}_b + S_{b,k} - S_{b,k\pm 1})$ Boundary wall,

$$(55)$$

$$\bar{q}_h = \frac{\bar{I}_y f_z - \bar{I}_{yz} f_y}{I_y I_z - I_{yz}^2} R - \frac{f_s}{F_s}, \quad (56)$$

$$\bar{q}_b = \frac{I_z f_y - I_{yz} f_z}{I_y I_z - I_{yz}^2} R \quad (57)$$

and

$$\bar{I}_y = I_y + \frac{z_s}{R} I_{yz},$$

$$\bar{I}_{yz} = I_{yz} + \frac{z_s}{R} I_z, \quad (56')$$

$$f_z = \int_0^s \frac{y t}{n} ds, \quad f_y = \int_0^s \frac{z t}{n} ds, \quad f_s = \int_0^s \frac{t}{n} ds. \quad (58)$$

Again both quantities $S_{h,k}$ and $S_{b,k}$ represent the terms respected to statically indeterminate shear flow.

By applying the principle of least work to that structure, the similar conditions to the Eq. (43) in paragraph 9 are obtained as follows:

$$\oint_k \frac{\check{q}_h n_g}{\rho t} ds = 0, \quad \oint_k \frac{\check{q}_b n_g}{\rho t} ds = 0.$$

Substituting the Eqs. (54) and (55) in these conditions, the following two sets of simultaneous equations for unknown quantities $S_{h,k}$ as well as $S_{b,k}$.

$$-S_{h,k-1} \int_{k,k-1} \frac{R^3 n_g}{\rho^3 t} ds + S_{h,k} \oint_k \frac{R^3 n_g}{\rho^3 t} ds - S_{h,k+1} \int_{k,k+1} \frac{R^3 n_g}{\rho^3 t} ds = - \oint_k \frac{R^3 \bar{q}_h n_g}{\rho^3 t} ds, \quad (59)$$

$$-S_{b,k-1} \int_{k,k-1} \frac{R^3 n_g}{\rho^3 t} ds + S_{b,k} \oint_k \frac{R^3 n_g}{\rho^3 t} ds - S_{b,k+1} \int_{k,k+1} \frac{R^3 n_g}{\rho^3 t} ds = - \oint_k \frac{R^3 \bar{q}_b n_g}{\rho^3 t} ds. \quad (60)$$

11. Shear Center

In general transverse loading condition, torsion always is produced in the curved girder simultaneously with bending.

In this case, if the shear center is not chosen as the center of torsion, both

bending moments and warping moment cannot be defined by such plainly formulae that have already been given in previous paragraph.

It is very important to know the position of the shear center S by this reason.

As shown in Fig. 19, let us adopt the coordinates (Y, Z) origin of which coincides with the shear center S . It is assumed that the position of the shear center are definitely decided by coordinates (y_s, z_s) and that both axes SY and SZ are parallel to the axes $0_n y$ and $0_n z$ respectively as shown in Fig. 19.

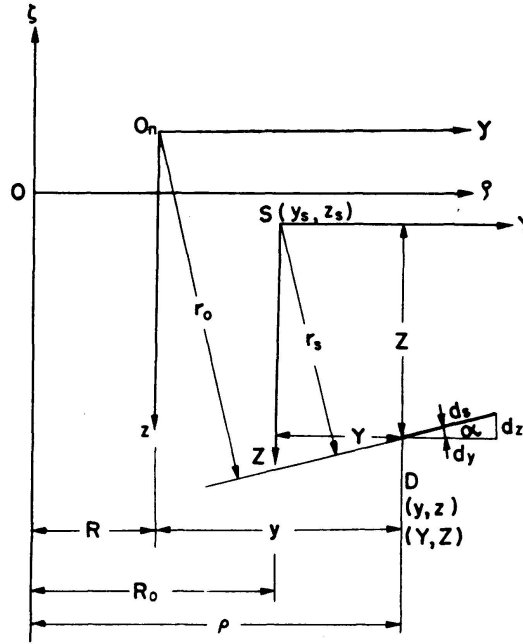


Fig. 19. Shear center.

Now, taking the point S as the center of torsion,

$$\int_0^s \frac{r_s}{\rho^2} ds = \int_0^s \frac{r_0}{\rho^2} ds - z_s \int_0^s \frac{dy}{\rho^2} + y_s \int_0^s \frac{dz}{\rho^2}, \quad (a)$$

where r_0 is the distance from the tangent at any point D to the middle line of the thin member to the centroid 0_n . The integral of the second and third terms of the above equation may be evaluated as follows:

$$\int_0^s \frac{dy(s)}{\rho^2} = \frac{y - y_0}{\rho \rho_0}, \quad \int_0^s \frac{dz(s)}{\rho^2} = \frac{1}{R} \left(\frac{z}{\rho} - \frac{z_0}{\rho_0} + \int_0^s \frac{r_0}{\rho^2} ds \right).$$

In above equation, y_0 , z_0 and ρ_0 denote the values of three kinds of coordinates y , z and ρ at the point $s=0$ from which s is measured respectively. Apply the above equation to the Eq. (a),

$$\int_0^s \frac{r_s}{\rho^2} ds = \frac{R_0}{R} \int_0^s \frac{r_0}{\rho^2} ds + y_s \frac{1}{R} \left(\frac{z}{\rho} - \frac{z_0}{\rho_0} \right) - z_s \frac{y - y_0}{\rho \rho_0}. \quad (b)$$

From Eq. (b), we readily obtain.

$$\oint_k \frac{r_s}{\rho^2} ds = \frac{R_0}{R} \oint_k \frac{r_0}{\rho^2} ds. \quad (c)$$

Substituting Eq. (c) in the right hand side of the Eq. (22), and putting

$$\tilde{q}_k = \frac{R_0}{R} \tilde{q}_{k,0}, \quad (61)$$

a set of simultaneous equations for $q_{k,0}$ will be obtained as follows:

$$-\tilde{q}_{k-1,0} \int_{k-1,k} \frac{R^3}{\rho^3} \frac{n_g}{t} ds + \tilde{q}_{k,0} \oint_k \frac{R^3}{\rho^3} \frac{n_g}{t} ds - \tilde{q}_{k+1,0} \int_{k,k+1} \frac{R^3}{\rho^3} \frac{n_g}{t} ds = R^2 \oint_k \frac{r_0}{\rho^2} ds. \quad (22')$$

By solving the Eq. (22)' to find $\tilde{q}_{k,0}$, the torsional function \tilde{q}_k may be evaluated by means of the Eq. (61).

Furthermore, substituting the Eqs. (b) and (61) into the Eq. (20), the warping function W_s at any point s will be found.

$$W_s = \frac{R_0}{R} \bar{W}_{s0} + \frac{R}{\rho} (z_s y - y_s z) + W_0, \quad (62)$$

$$\begin{aligned} \text{where } \bar{W}_{s0} &= \int_0^s \frac{R^3}{\rho^3} \frac{n_g}{t} \tilde{q}_{k,0} ds - R^2 \int_0^s \frac{r_0}{\rho^2} ds && \text{Nonboundary wall,} \\ &= \int_0^s \frac{R^3}{\rho^3} \frac{n_g}{t} (\tilde{q}_{k,0} - \tilde{q}_{k\pm 1,0}) ds - R^2 \int_0^s \frac{r_0}{\rho^2} ds && \text{Boundary wall.} \end{aligned} \quad (63)$$

W_0 represents the value of W_s at $s=0$, and should be determined by the following conditions. The stress-system σ_w of this type is set up, which consists of self-equilibrating stress-systems which are called axial constraint stresses. Therefore no axial force is produced due to secondary stress σ_w , so

$$\int_F \sigma_w dF = 0. \quad (d)$$

Substituting the Eq. (62) in the Eq. (d), W_0 will be

$$W_0 = \frac{-R_0}{R} \frac{\int_F \bar{W}_{s0} \frac{t}{n} ds}{F_s} \quad (64)$$

Because of self-equilibrating stress-systems, no bending moment about two mutually perpendicular coordinate axes also is produced due to secondary normal stress σ_w ,

$$\int_F \sigma_w y dF = 0, \quad \int_F \sigma_w z dF = 0. \quad (e)$$

By means of the condition (e), the following system of equations will be obtained.

$$\begin{aligned}(I_{yz} - B_z)y_s - I_z z_s &= C_z, \\ (I_y - B_y)y_s - I_{yz} z_s &= C_y,\end{aligned}\quad (65)$$

where

$$C_y = \int_F \frac{W_{s0} z t}{n} ds, \quad C_z = \int_F \frac{W_{s0} y t}{n} ds, \quad (66)$$

$$B_y = \frac{C_y}{R}, \quad B_z = \frac{C_z}{R}, \quad (67)$$

$$W_{s0} = \bar{W}_{s0} + W_0 \frac{R}{R_0}. \quad (68)$$

Finally, the coordinates of the shear center S is given by the following equations.

$$y_s = \frac{C_y I_z - C_z I_{yz}}{I_z(I_y - B_y) - I_{yz}(I_{yz} - B_z)}, \quad z_s = \frac{C_y(I_{yz} - B_z) - C_z(I_y - B_y)}{I_z(I_y - B_y) - I_{yz}(I_{yz} - B_z)}. \quad (69)$$

12. Deformation

If the curved girder is subjected to the vertical load, in general the whole cross section will undergo vertical translation of and rotation about the shear center S .

The assumed positive directions for the deflection δ and the angle of rotation β are given in Fig. 20.

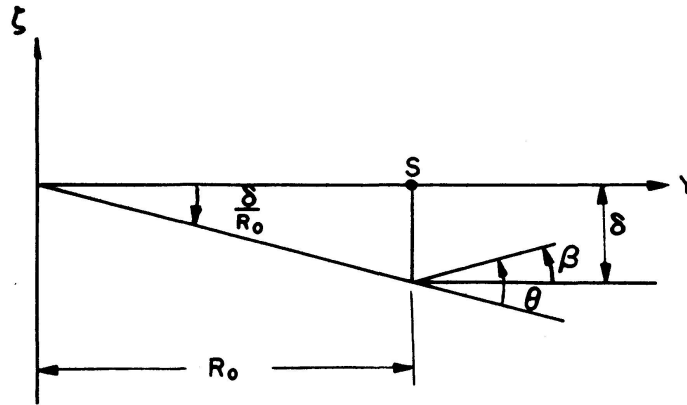


Fig. 20. Deformation.

It may be clear from the fundamental condition of deformation, namely, pure torsion, pure bending normal to and in the initial curvature, that the torsional angle θ is expressed by the following formula.

$$\theta = \beta + \frac{\delta}{R_0}, \quad (70)$$

where the positive direction for θ is also given in Fig. 20.

While the displacement of shear center v_0 in the ζ direction may be found by putting $Y = 0, \rho = R_0$ in the Eqs. (7) and (26), and superimposing them up.

$$v_0 = R_0 \left\{ \int_0^\varphi \sin(\varphi - \varphi') \frac{d\gamma}{d\varphi'} d\varphi' - \int_0^\varphi [1 - \cos(\varphi - \varphi')] \frac{d\theta}{d\varphi'} d\varphi' \right\}.$$

By using the above equation, the following equation can be easily introduced.

$$\frac{d^2 v_0}{d\varphi^2} + v_0 = R_0 \left(\frac{d\gamma}{d\varphi} - \theta \right).$$

Taking into account the relation $v_0 = -\delta$,

$$\frac{d^2 \delta}{d\varphi^2} + \delta = R_0 \left(\theta - \frac{d\gamma}{d\varphi} \right). \quad (71)$$

II. Three Dimensional Analysis of Curved Girder

1. Relations Between Stress Resultants and External Forces of Curved Girder Bridges

Let us now introduce the relations between the stress resultants at whole bridge section and the external forces for the curved girder bridge under the distributed vertical load $p(\rho, \varphi)$ and horizontal load $p_h(\varphi)$.

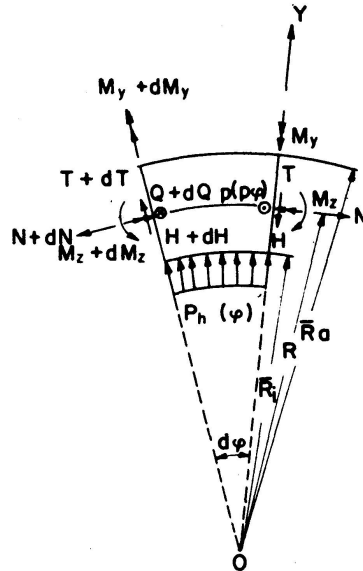


Fig. 1. Stress resultants and external forces.

Every stress resultant, namely, two bending moments M_y, M_z about two mutually perpendicular axes $0_n y$ and $0_n z$, a torsional moment T , two shearing forces Q, H in two direction $0_n z, 0_n y$, and a axial force N are assumed to be positive in such direction as shown in Fig. 1.

The statical equilibrium should be considered for differential elements cut out by a pair of neighbouring radial section having a differential angle $d\varphi$.

a) *Equilibrium of Forces in the Z-direction*

$$\frac{dQ}{d\varphi} = - \int_{\bar{R}_i}^{\bar{R}_a} p(\rho, \varphi) \rho d\rho, \quad (1)$$

where \bar{R}_i and \bar{R}_a are the horizontal distance from the center of curvature 0 to the inner and outer side of the distributed vertical load, respectively.

b) *Equilibrium of Forces in the Peripheral Direction*

$$\frac{dN}{d\varphi} = -H. \quad (2)$$

c) *Equilibrium of Forces in the Y-direction*

$$\frac{dH}{d\varphi} + p_h(\varphi) - N = 0. \quad (3)$$

d) *Equilibrium of Moments About the Shear Center*

$$\frac{dT}{d\varphi} = M_y + \int_{\bar{R}_i}^{\bar{R}_a} p(\rho, \varphi) Y \rho d\rho - p_h(\varphi) Z_h - N z_s, \quad (4)$$

where Z_h is the vertical distance between the shear center and the load p_h .

e) *Equilibrium of Moments About the Axis $O_n y$*

$$\frac{dM_y}{d\varphi} = Q R_0 - T - H z_s. \quad (5)$$

f) *Equilibrium of Moments About the Axis $O_n z$*

$$\frac{dM_z}{d\varphi} = H R. \quad (6)$$

Firstly eliminating both H and N from the Eqs. (2), (3), and (6), a following differential equation for M_z can be readily obtained.

$$\frac{d^3 M_z}{d\varphi^3} + \frac{dM_z}{d\varphi} = -R \frac{dp_h}{d\varphi}. \quad (7)$$

Next, eliminating both T and Q from the Eq. (1), (4), and (5), a following differential equation for M_y can also be obtained. Putting $z_h = Z_h + z_s$,

$$\frac{d^2 M_y}{d\varphi^2} + M_y = p_h z_h - \int_{\bar{R}_i}^{\bar{R}_a} p \rho^2 d\rho. \quad (8)$$

In similar way, eliminating H from the Eqs. (2) and (3), the differential equation for N can be given as follows:

$$\frac{d^2 N}{d\varphi^2} + N = p_h. \quad (9)$$

Consequently, by solving these three differential equations simultaneously under given vertical load p and horizontal load p_h , two bending moments about mutually perpendicular axes and a axial force can be plainly found. In a special case when only vertical load acts on the girder, as the quantities p_h and N vanish, the solution for M_y can be found independently of any other equations.

2. Solutions for the Simply Supported Curved Girder Bridge Under Several Typical Loading

The differential Eq. (8) has been solved for six typical loading conditions as shown in Fig. 2, and various kinds of stress resultants and deformations will be found on the basis of those solutions.

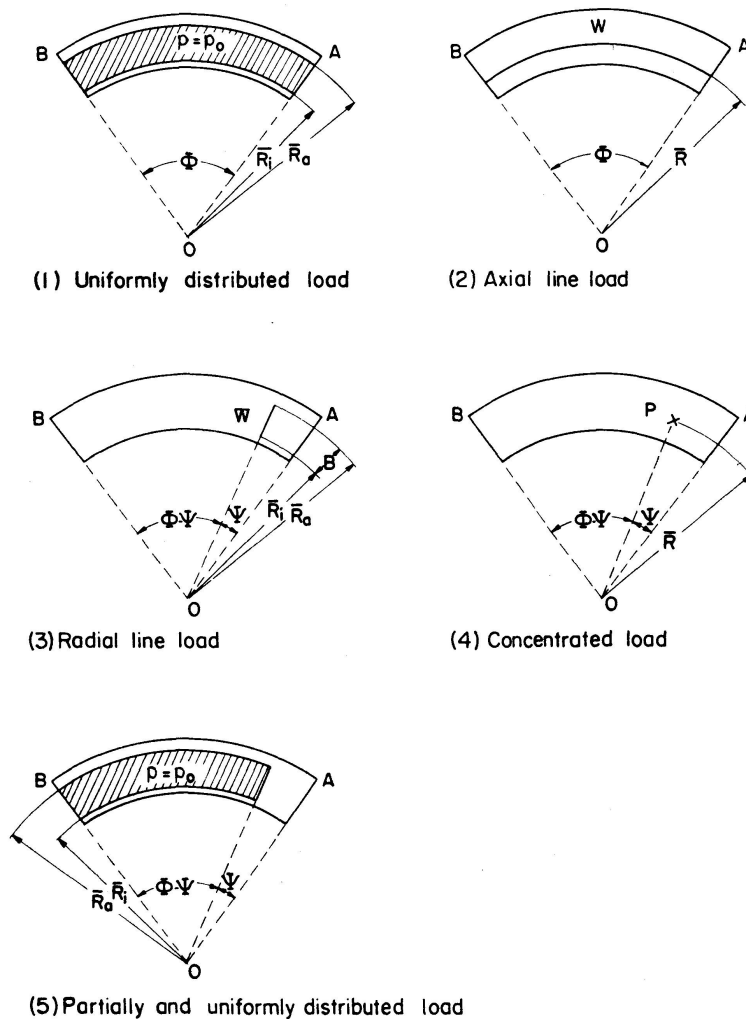


Fig. 2. Typical vertical load.

a) *Bending Moment M_y*

The solutions have been obtained for bending moment M_y as shown in Table 1. Where,

$$L_1 = \frac{1}{3}(\bar{R}_a^3 - \bar{R}_i^3), \quad L_2 = \frac{R_0}{2}(\bar{R}_a^2 - \bar{R}_i^2). \quad (10)$$

Table 1. Solution for bending moment M_y

(1)	$L_1 p_0 \left[\frac{\sin \varphi + \sin (\Phi - \varphi)}{\sin \Phi} - 1 \right]$
(2)	$\bar{R}^2 W \left[\frac{\sin \varphi + \sin (\Phi - \varphi)}{\sin \Phi} - 1 \right]$
(3)	$\frac{L_2}{R_0} W \frac{\sin (\Phi - \Psi)}{\sin \Phi} \sin \varphi, \quad 0 \leq \varphi \leq \Psi$ $\frac{L_2}{R_0} W \frac{\sin (\Phi - \varphi)}{\sin \Phi} \sin \Psi, \quad \Psi \leq \varphi \leq \Phi$
(4)	$\bar{R} P \frac{\sin (\Phi - \Psi)}{\sin \Phi} \sin \varphi, \quad 0 \leq \varphi \leq \Psi$ $\bar{R} P \frac{\sin (\Phi - \varphi)}{\sin \Phi} \sin \Psi, \quad \Psi \leq \varphi \leq \Phi$
(5)	$L_1 p_0 \frac{1 - \cos (\Phi - \Psi)}{\sin \Phi} \sin \varphi, \quad 0 \leq \varphi \leq \Psi$ $L_1 p_0 \left[\frac{\sin \varphi + \sin (\Phi - \varphi) \cos \Psi}{\sin \Phi} - 1 \right], \quad \Psi \leq \varphi \leq \Phi$
(6)	$-m_T \frac{\sin (\Phi - \Psi)}{\sin \Phi} \sin \varphi, \quad 0 \leq \varphi \leq \Psi$ $-m_T \frac{\sin (\Phi - \varphi)}{\sin \Phi} \sin \Psi, \quad \Psi \leq \varphi \leq \Phi$

The loading condition (6) corresponds to the case when the concentrated torque m_T about the axis of shear center acts at the position $\varphi = \psi$.

Where m_T is assumed to be positive in the case when the girder inclines inward.

If not any horizontal load acts on the girder, the axial force N and bending moment M_z will not be evidently produced.

b) *Warping Moment M_w*

In every loading condition shown in Fig. 2, both P_h and N in the relation (4) will vanish, so that

$$\frac{dT}{d\varphi} = M_y + \int_{\bar{R}_i}^{\bar{R}_a} p Y \rho d\rho. \quad (11)$$

On the other hand, it may be fairly recognized that there is the relation (4) between the warping moment M_w and torsional moment T .

$$\frac{d^2 M_w}{d\varphi^2} - \frac{G_s J}{E_s C_w} R^2 M_w = -R \frac{dT}{d\varphi}. \quad (12)$$

By using the Eqs. (11) and (12), the differential equation for M_w can be readily obtained.

$$\frac{d^2 M_w}{d\varphi^2} - \alpha^2 M_w = -R \left(M_y + \int_{\bar{R}_i}^{\bar{R}_a} p Y \rho d\rho \right). \quad (13)$$

where

$$\alpha = R \sqrt{\frac{G_s J}{E_s C_w}}. \quad (14)$$

Table 2. Solutions for warping moment M_w

(1)	$R p_0 \left\{ \frac{L_1}{\alpha^2 + 1} \frac{\sin \varphi + \sin (\Phi - \varphi)}{\sin \Phi} - \left(\frac{L_1}{\alpha^2 + 1} - \frac{L_2}{\alpha^2} \right) \frac{\sinh \alpha \varphi + \sinh \alpha (\Phi - \varphi)}{\sin \alpha \Phi} - \frac{L_2}{\alpha^2} \right\}$
(2)	$R W \left\{ \frac{\bar{R}^2}{\alpha^2 + 1} \frac{\sin \varphi + \sin (\Phi - \varphi)}{\sin \Phi} - \left(\frac{\bar{R}^2}{\alpha^2 + 1} - \frac{\bar{R} R_0}{\alpha^2} \right) \frac{\sinh \alpha \varphi + \sinh \alpha (\Phi - \varphi)}{\sin \alpha \Phi} - \frac{\bar{R} R_0}{\alpha^2} \right\}$
(3)	$\frac{R}{R_0} W \left\{ \left(\frac{L_2}{\alpha^2 + 1} - \frac{L_3}{\alpha^2} \right) \alpha \frac{\sinh \alpha (\Phi - \Psi)}{\sinh \alpha \Phi} \sinh \alpha \varphi + \frac{L_2}{\alpha^2 + 1} \frac{\sin (\Phi - \Psi)}{\sin \Phi} \sin \varphi \right\}, \quad 0 \leq \varphi \leq \Psi$ $\frac{R}{R_0} W \left\{ \left(\frac{L_2}{\alpha^2 + 1} - \frac{L_3}{\alpha^2} \right) \alpha \frac{\sinh \alpha (\Phi - \varphi)}{\sinh \alpha \Phi} \sinh \alpha \Psi + \frac{L_2}{\alpha^2 + 1} \frac{\sin (\Phi - \varphi)}{\sin \Phi} \sin \Psi \right\}, \quad \Psi \leq \varphi \leq \Phi$
(4)	$R P \left\{ \left(\frac{\bar{R}}{\alpha^2 + 1} - \frac{R_0}{\alpha^2} \right) \alpha \frac{\sinh \alpha (\Phi - \Psi)}{\sinh \alpha \Phi} \sinh \alpha \varphi + \frac{\bar{R}}{\alpha^2 + 1} \frac{\sin (\Phi - \Psi)}{\sin \Phi} \sin \varphi \right\}, \quad 0 \leq \varphi \leq \Psi$ $R P \left\{ \left(\frac{\bar{R}}{\alpha^2 + 1} - \frac{R_0}{\alpha^2} \right) \alpha \frac{\sinh \alpha (\Phi - \varphi)}{\sinh \alpha \Phi} \sinh \alpha \Psi + \frac{\bar{R}}{\alpha^2 + 1} \frac{\sin (\Phi - \varphi)}{\sin \Phi} \sin \Psi \right\}, \quad \Psi \leq \varphi \leq \Phi$
(5)	$R p_0 \left\{ \left(\frac{L_1}{\alpha^2 + 1} - \frac{L_2}{\alpha^2} \right) \frac{\cosh \alpha (\Phi - \Psi) - 1}{\sinh \alpha \Phi} \sinh \alpha \varphi + \frac{L_1}{\alpha^2 + 1} \frac{1 - \cos (\Phi - \Psi)}{\sin \Phi} \sin \varphi \right\},$ $0 \leq \varphi \leq \Psi$ $R p_0 \left\{ \frac{L_1}{\alpha^2 + 1} \frac{\sin \varphi + \sin (\Phi - \varphi) \cos \Psi}{\sin \Phi} - \left(\frac{L_1}{\alpha^2 + 1} - \frac{L_2}{\alpha^2} \right) \frac{\sinh \alpha \varphi + \sinh \alpha (\Phi - \varphi) \cosh \alpha \Psi}{\sinh \alpha \Phi} - \frac{L_2}{\alpha^2} \right\}, \quad \Psi \leq \varphi \leq \Phi$
(6)	$-m_T \frac{R}{\alpha^2 + 1} \left[\alpha \frac{\sinh \alpha (\Phi - \Psi)}{\sinh \alpha \Phi} \sinh \alpha \varphi + \frac{\sin (\Phi - \Psi)}{\sin \Phi} \sin \varphi \right], \quad 0 \leq \varphi \leq \Psi$ $-m_T \frac{R}{\alpha^2 + 1} \left[\alpha \frac{\sinh \alpha (\Phi - \varphi)}{\sinh \alpha \Phi} \sinh \alpha \Psi + \frac{\sin (\Phi - \varphi)}{\sin \Phi} \sin \Psi \right], \quad \Psi \leq \varphi \leq \Phi$

The solutions of the above differential Eq. (13) under various loading conditions are found as shown in Table 2, where

$$L_3 = R_0^2 (\bar{R}_a - \bar{R}_i). \quad (15)$$

c) *Torsional Angle θ*

The torsional angle θ may be readily obtained by integrating twice the expression of M_w , that is

$$\theta = \iint \frac{M_w}{E_s C_w} R^2 (d\varphi)^2 + A\varphi + B, \quad (16)$$

where A and B are the integral constants and are determined by the boundary conditions.

The results are shown in Table 3.

d) *Angle of Rotation β of Section*

The differential equation for angle of rotation β of section becomes as follows:

$$\frac{d^2\beta}{d\varphi^2} + \beta = M_w \frac{R^2}{E_s C_w} + M_y \frac{R}{E_s I'_y}, \quad (17)$$

where
$$I'_y = I_y - \frac{I_{yz}^2}{I_z}. \quad (18)$$

The terms including M_y and M_w in the right-hand side of the Eq. (17) have been already known as the function of available φ and given in Table 1 and 2.

By using these value, β may be found for the same typical conditions as shown in Table 4. The constants κ_1 , κ_2 and κ_3 included in Table 4 have the following values.

$$\kappa_1 = \left[\frac{R^2}{E_s C_w (\alpha^2 + 1)} + \frac{1}{E_s I'_y} \right] \frac{L_1}{2}, \quad (19-1)$$

$$\kappa_2 = \frac{R^2}{E_s C_w (\alpha^2 + 1)} \left(\frac{L_1}{\alpha^2 + 1} - \frac{L_2}{\alpha^2} \right), \quad (19-2)$$

$$\kappa_3 = \frac{R^2 L_2}{E_s C_w \alpha^2} + \frac{L_1}{E_s I'_y}. \quad (19-3)$$

The constants μ_1 , μ_2 and μ_3 are given by putting $L_1 = \bar{R}^2$, $L_2 = R_0 \bar{R}$ in κ_1 , κ_2 and κ_3 respectively. Moreover, the constants ν_1 and ν_2 is given by

$$\nu_1 = \left[\frac{R^2}{E_s C_w (\alpha^2 + 1)} + \frac{1}{E_s I'_y} \right] \frac{L_2}{2}, \quad (20-1)$$

$$\nu_2 = \frac{R^2}{E_s C_w (\alpha^2 + 1)} \left(\frac{L_2}{\alpha^2 + 1} - \frac{L_3}{\alpha^2} \right). \quad (20-2)$$

e) *Deflection δ*

The deflection δ of shear center at any cross section may be found from the results of tables (3) and (4) by the following formula, $\delta = R_0 (\theta - \beta)$.

The solutions for δ under the same typical loading conditions are given in Table 5.

Table 3. Solutions for torsional angle θ

(1)	$\frac{R p_0}{G_s J} \left\{ \left(\frac{L_2}{\alpha^2} - \frac{L_1}{\alpha^2 + 1} \right) \frac{\sinh \alpha \varphi + \sinh \alpha (\Phi - \varphi)}{\sinh \alpha \Phi} - \frac{L_1}{\alpha^2 + 1} \alpha^2 \frac{\sin \varphi + \sin (\Phi - \varphi)}{\sin \Phi} \right. \\ \left. + \frac{L_2}{\alpha^2} \left(\frac{\alpha^2 \Phi \varphi}{2} - \frac{\alpha^2 \varphi^2}{2} - 1 \right) + L_1 \right\}$
(2)	$\frac{R W}{G_s J} \left\{ \left(\frac{R_0}{\alpha^2} - \frac{\bar{R}}{\alpha^2 + 1} \right) \bar{R} \frac{\sinh \alpha \varphi + \sinh \alpha (\Phi - \varphi)}{\sinh \alpha \Phi} - \frac{\bar{R}^2}{\alpha^2 + 1} \alpha^2 \frac{\sin \varphi + \sin (\Phi - \varphi)}{\sin \Phi} \right. \\ \left. + \frac{R_0 \bar{R}}{\alpha^2} \left(\frac{\alpha^2 \Phi \varphi}{2} - \frac{\alpha^2 \varphi^2}{2} - 1 \right) + \bar{R}^2 \right\}$
(3)	$\frac{R W}{R_0 G_s J} \left\{ \left(\frac{L_2}{\alpha^2 + 1} - \frac{L_3}{\alpha^2} \right) \alpha \frac{\sinh \alpha (\Phi - \Psi)}{\sinh \alpha \Phi} \sinh \alpha \varphi \right. \\ \left. - \frac{L_2}{\alpha^2 + 1} \alpha^2 \frac{\sin (\Phi - \Psi)}{\sin \Phi} \sin \varphi + L_3 \frac{\Phi - \Psi}{\Phi} \varphi \right\}, \quad 0 \leq \varphi \leq \Psi$ $\frac{R W}{R_0 G_s J} \left\{ \left(\frac{L_2}{\alpha^2 + 1} - \frac{L_3}{\alpha^2} \right) \alpha \frac{\sinh \alpha (\Phi - \varphi)}{\sinh \alpha \Phi} \sinh \alpha \Psi \right. \\ \left. - \frac{L_2}{\alpha^2 + 1} \alpha^2 \frac{\sin (\Phi - \varphi)}{\sin \Phi} \sin \Psi + L_3 \frac{\Phi - \varphi}{\Phi} \Psi \right\}, \quad \Psi \leq \varphi \leq \Phi$
(4)	$\frac{R P}{G_s J} \left\{ \left(\frac{\bar{R}}{\alpha^2 + 1} - \frac{R_0}{\alpha^2} \right) \alpha \frac{\sinh \alpha (\Phi - \Psi)}{\sinh \alpha \Phi} \sinh \alpha \varphi \right. \\ \left. - \frac{\bar{R}}{\alpha^2 + 1} \alpha^2 \frac{\sin (\Phi - \Psi)}{\sin \Phi} \sin \varphi + R_0 \frac{\Phi - \Psi}{\Phi} \varphi \right\}, \quad 0 \leq \varphi \leq \Psi$ $\frac{R P}{G_s J} \left\{ \left(\frac{\bar{R}}{\alpha^2 + 1} - \frac{R_0}{\alpha^2} \right) \alpha \frac{\sinh \alpha (\Phi - \varphi)}{\sinh \alpha \Phi} \sinh \alpha \Psi \right. \\ \left. - \frac{\bar{R}_1}{\alpha^2 + 1} \alpha^2 \frac{\sin (\Phi - \varphi)}{\sin \Phi} \sin \Psi + R_0 \frac{\Phi - \varphi}{\Phi} \Psi \right\}, \quad \Psi \leq \varphi \leq \Phi$
(5)	$\frac{R p_0}{G_s J} \left\{ \left(\frac{L_1}{\alpha^2 + 1} - \frac{L_2}{\alpha^2} \right) \frac{\cosh \alpha (\Phi - \Psi) - 1}{\sinh \alpha \Phi} \sinh \alpha \varphi \right. \\ \left. - \frac{L_1}{\alpha^2 + 1} \alpha^2 \frac{1 - \cos (\Phi - \Psi)}{\sin \Phi} \sin \varphi + \frac{L_2}{2 \Phi} (\Phi - \Psi)^2 \varphi \right\}, \quad 0 \leq \varphi \leq \Psi$ $\frac{R p_0}{G_s J} \left\{ \left(\frac{L_2}{\alpha^2} - \frac{L_1}{\alpha^2 + 1} \right) \frac{\sinh \alpha \varphi + \sinh \alpha (\Phi - \varphi) \cosh \alpha \Psi}{\sinh \alpha \Phi} \right. \\ \left. - \frac{L_1}{\alpha^2 + 1} \alpha^2 \frac{\sin \varphi + \sin (\Phi - \varphi) \cos \Psi}{\sin \Phi} - \frac{L_2}{2} (\varphi - \Psi)^2 + \frac{\varphi}{2 \Phi} L_2 (\Phi - \Psi)^2 + L_1 - \frac{L_2}{\alpha^2} \right\}, \\ \Psi \leq \varphi \leq \Phi$
(6)	$-m_T \frac{R \alpha}{G_s J (\alpha^2 + 1)} \left\{ \frac{\sinh \alpha (\Phi - \Psi)}{\sinh \alpha \Phi} \sinh \alpha \varphi - \alpha \frac{\sin (\Phi - \Psi)}{\sin \Phi} \sin \varphi \right\}, \quad 0 \leq \varphi \leq \Psi$ $-m_T \frac{R \alpha}{G_s J (\alpha^2 + 1)} \left\{ \frac{\sinh \alpha (\Phi - \varphi)}{\sinh \alpha \Phi} \sinh \alpha \Psi - \alpha \frac{\sin (\Phi - \varphi)}{\sin \Phi} \sin \Psi \right\}, \quad \Psi \leq \varphi \leq \Phi$

Table 4. Solutions for angle of rotation β of section, $\lambda = (R^2/L_1) \kappa_1$

(1)	$R p_0 \left\{ \kappa_1 \left[\frac{1 - \cos \Phi}{\sin \Phi} \left(\Phi \cos \Phi \frac{\sin \varphi}{\sin \Phi} - \varphi \cos \varphi \right) + (\varphi - \Phi) \sin \varphi \right] \right.$ $\left. + \kappa_2 \left[\frac{\sin \varphi + \sin (\Phi - \varphi)}{\sin \Phi} - \frac{\sinh \alpha \varphi + \sinh \alpha (\Phi - \varphi)}{\sinh \alpha \Phi} \right] + \kappa_3 \left[\frac{\sin \varphi + \sin (\Phi - \varphi)}{\sin \Phi} - 1 \right] \right\}$
(2)	$R W \left\{ \mu_1 \left[\frac{1 - \cos \Phi}{\sin \Phi} \left(\Phi \cos \Phi \frac{\sin \varphi}{\sin \Phi} - \varphi \cos \varphi \right) + (\varphi - \Phi) \sin \varphi \right] \right.$ $\left. + \mu_2 \left[\frac{\sin \varphi + \sin (\Phi - \varphi)}{\sin \Phi} - \frac{\sinh \alpha \varphi + \sinh \alpha (\Phi - \varphi)}{\sinh \alpha \Phi} \right] + \mu_3 \left[\frac{\sin \varphi + \sin (\Phi - \varphi)}{\sin \Phi} - 1 \right] \right\}$
(3)	$\frac{R}{R_0} W \left\{ \nu_1 \left[\frac{\sin (\Phi - \Psi)}{\sin \Phi} \left(\Phi \cos \Phi \frac{\sin \varphi}{\sin \Phi} - \varphi \cos \varphi \right) + (\sin \overline{\Phi - \Psi} - \overline{\Phi - \Psi} \cos \overline{\Phi - \Psi}) \frac{\sin \varphi}{\sin \Phi} \right] \right.$ $\left. + \nu_2 \alpha \left[\frac{\sinh \alpha (\Phi - \Psi)}{\sinh \alpha \Phi} \sinh \alpha \varphi - \alpha \sin (\Phi - \Psi) \frac{\sin \varphi}{\sin \Phi} \right] \right\}, \quad 0 \leq \varphi \leq \Psi$ $\frac{R}{R_0} W \left\{ \nu_1 \left[\frac{\sin (\Phi - \varphi)}{\sin \Phi} \left(\Phi \cos \Phi \frac{\sin \Psi}{\sin \Phi} - \Psi \cos \Psi \right) + (\sin \overline{\Phi - \varphi} - \overline{\Phi - \varphi} \cos \overline{\Phi - \varphi}) \frac{\sin \Psi}{\sin \Phi} \right] \right.$ $\left. + \nu_2 \alpha \left[\frac{\sinh \alpha (\Phi - \varphi)}{\sinh \alpha \Phi} \sinh \alpha \Psi - \alpha \sin (\Phi - \varphi) \frac{\sin \Psi}{\sin \Phi} \right] \right\}, \quad \Psi \leq \varphi \leq \Phi$
(4)	$\frac{R P}{\bar{R}} \left\{ \mu_1 \left[\frac{\sin (\Phi - \Psi)}{\sin \Phi} \left(\Phi \cos \Phi \frac{\sin \varphi}{\sin \Phi} - \varphi \cos \varphi \right) + (\sin \overline{\Phi - \Psi} - \overline{\Phi - \Psi} \cos \overline{\Phi - \Psi}) \frac{\sin \varphi}{\sin \Phi} \right] \right.$ $\left. + \mu_2 \alpha \left[\frac{\sinh \alpha (\Phi - \Psi)}{\sinh \alpha \Phi} \sinh \alpha \varphi - \alpha \sin (\Phi - \Psi) \frac{\sin \varphi}{\sin \Phi} \right] \right\}, \quad 0 \leq \varphi \leq \Psi$ $\frac{R P}{\bar{R}} \left\{ \mu_1 \left[\frac{\sin (\Phi - \varphi)}{\sin \Phi} \left(\Phi \cos \Phi \frac{\sin \Psi}{\sin \Phi} - \Psi \cos \Psi \right) + (\sin \overline{\Phi - \varphi} - \overline{\Phi - \varphi} \cos \overline{\Phi - \varphi}) \frac{\sin \Psi}{\sin \Phi} \right] \right.$ $\left. + \mu_2 \alpha \left[\frac{\sinh \alpha (\Phi - \varphi)}{\sinh \alpha \Phi} \sinh \alpha \Psi - \alpha \sin (\Phi - \varphi) \frac{\sin \Psi}{\sin \Phi} \right] \right\}, \quad \Psi \leq \varphi \leq \Phi$
(5)	$R p_0 \left\{ \frac{\kappa_1}{\sin \Phi} \left[(\cos \Phi - \cos \Psi) \Phi \frac{\sin \varphi}{\sin \Phi} + \varphi \cos \varphi (\cos \overline{\Phi - \Psi} - 1) + \Psi \sin (\Phi - \Psi) \sin \varphi \right] \right.$ $\left. + \kappa_2 \left[\frac{\cosh \alpha (\Phi - \Psi) - 1}{\sinh \alpha \Phi} \sinh \alpha \varphi + \frac{\sin \varphi}{\sin \Phi} (1 - \cos \overline{\Phi - \Psi}) \right] + \kappa_3 [1 - \cos (\Phi - \Psi)] \frac{\sin \varphi}{\sin \Phi} \right\},$ $0 \leq \varphi \leq \Psi$ $R p_0 \left\{ \frac{\kappa_1}{\sin \Phi} \left[(\cos \Phi - \cos \Psi) \Phi \frac{\sin \varphi}{\sin \Phi} - \varphi \cos \varphi + \varphi \cos (\Phi - \varphi) \cos \Psi + \Psi \sin (\Phi - \varphi) \sin \Psi \right] \right.$ $\left. + \kappa_2 \left[\frac{\sin \varphi + \sin (\Phi - \varphi) \cos \Psi}{\sin \Phi} - \frac{\sinh \alpha \varphi + \sinh \alpha (\Phi - \varphi) \cosh \alpha \Psi}{\sinh \alpha \Phi} \right] \right.$ $\left. + \kappa_3 \left[\frac{\sin \varphi}{\sin \Phi} + \sin (\Phi - \varphi) \frac{\cos \Psi}{\sin \Phi} - 1 \right] \right\}, \quad \Psi \leq \varphi \leq \Phi$
(6)	$-m_T \left\{ \frac{\lambda}{R} \left[\frac{\sin (\Phi - \Psi)}{\sin \Phi} \left(\Phi \cos \Phi \frac{\sin \varphi}{\sin \Phi} - \varphi \cos \varphi \right) + (\sin \overline{\Phi - \Psi} - \overline{\Phi - \Psi} \cos \overline{\Phi - \Psi}) \frac{\sin \varphi}{\sin \Phi} \right] \right.$ $\left. + \frac{R^3 \alpha}{E_s C_w (\alpha^2 + 1)^2} \left[\frac{\sinh \alpha (\Phi - \Psi)}{\sinh \alpha \Phi} \sinh \alpha \varphi - \alpha \frac{\sin (\Phi - \Psi)}{\sin \Phi} \sin \varphi \right] \right\}, \quad 0 \leq \varphi \leq \Psi$ $-m_T \left\{ \frac{\lambda}{R} \left[\frac{\sin (\Phi - \varphi)}{\sin \Phi} \left(\Phi \cos \Phi \frac{\sin \Psi}{\sin \Phi} - \Psi \cos \Psi \right) + (\sin \overline{\Phi - \varphi} - \overline{\Phi - \varphi} \cos \overline{\Phi - \varphi}) \frac{\sin \Psi}{\sin \Phi} \right] \right.$ $\left. + \frac{R^3 \alpha}{E_s C_w (\alpha^2 + 1)^2} \left[\frac{\sinh \alpha (\Phi - \varphi)}{\sinh \alpha \Phi} \sinh \alpha \Psi - \alpha \frac{\sin (\Phi - \varphi)}{\sin \Phi} \sin \Psi \right] \right\}, \quad \Psi \leq \varphi \leq \Phi$

Table 5. Solutions for deflections δ

$$\omega_1 = \frac{L_1 \alpha^2}{G_s J (\alpha^2 + 1)} + \kappa_1 + \kappa_2, \quad \omega_2 = \frac{\bar{R}^2 \alpha^2}{G_s J (\alpha^2 + 1)} + \mu_1 + \mu_2$$

(1)	$R_0 R p_0 \left\{ -\frac{\kappa^2}{\alpha^2} \frac{\sinh \alpha \varphi + \sinh \alpha (\Phi - \varphi)}{\sinh \alpha \Phi} - \omega_1 \frac{\sin \varphi + \sin (\Phi - \varphi)}{\sin \Phi} \right.$ $+ \frac{1}{G_s J} \left[\frac{L_2}{\alpha^2} \left(\frac{\alpha^2 \varphi \Phi}{2} - \frac{\alpha^2 \varphi^2}{2} - 1 \right) + L_1 \right]$ $\left. - \kappa_1 \left[\frac{1 - \cos \Phi}{\sin \Phi} \left(\Phi \cos \Phi \frac{\sin \varphi}{\sin \Phi} - \varphi \cos \varphi \right) + (\varphi - \Phi) \sin \varphi \right] + \kappa_3 \right\}$
(2)	$R_0 R W \left\{ -\frac{\mu_2}{\alpha^2} \frac{\sinh \alpha \varphi + \sinh \alpha (\Phi - \varphi)}{\sinh \alpha \Phi} - \omega_2 \frac{\sin \varphi + \sin (\Phi - \varphi)}{\sin \Phi} \right.$ $+ \frac{1}{G_s J} \left[\frac{R_0 \bar{R}}{\alpha^2} \left(\frac{\alpha^2 \varphi \Phi}{2} - \frac{\alpha^2 \varphi^2}{2} - 1 \right) + \bar{R}^2 \right]$ $\left. - \mu_1 \left[\frac{1 - \cos \Phi}{\sin \Phi} \left(\Phi \cos \Phi \frac{\sin \varphi}{\sin \Phi} - \varphi \cos \varphi \right) + (\varphi - \Phi) \sin \varphi \right] + \mu_3 \right\}$
(3)	$R W \left\{ \frac{\nu_2}{\alpha} \frac{\sinh \alpha (\Phi - \Psi)}{\sinh \alpha \Phi} \sinh \alpha \varphi + \alpha^2 \left[\nu_2 - \frac{L_2}{G_s J (\alpha^2 + 1)} \right] \frac{\sin (\Phi - \Psi)}{\sin \Phi} \sin \varphi \right.$ $- \nu_1 \left[\frac{\sin (\Phi - \Psi)}{\sin \Phi} \left(\Phi \cos \Phi \frac{\sin \varphi}{\sin \Phi} - \varphi \cos \varphi \right) \right.$ $\left. + (\sin \overline{\Phi - \Psi} - \overline{\Phi - \Psi} \cos \overline{\Phi - \Psi}) \frac{\sin \varphi}{\sin \Phi} \right] + \frac{L_3}{G_s J} \frac{\Phi - \Psi}{\Phi} \varphi \Big\}, \quad 0 \leq \varphi \leq \Psi$ $R W \left\{ \frac{\nu_2}{\alpha} \frac{\sinh \alpha (\Phi - \varphi)}{\sinh \alpha \Phi} \sinh \alpha \Psi + \alpha^2 \left[\nu_2 - \frac{L_2}{G_s J (\alpha^2 + 1)} \right] \frac{\sin (\Phi - \varphi)}{\sin \Phi} \sin \Psi \right.$ $- \nu_1 \left[\frac{\sin (\Phi - \varphi)}{\sin \Phi} \left(\Phi \cos \Phi \frac{\sin \Psi}{\sin \Phi} - \Psi \cos \Psi \right) \right.$ $\left. + (\sin \overline{\Phi - \varphi} - \overline{\Phi - \varphi} \cos \overline{\Phi - \varphi}) \frac{\sin \Psi}{\sin \Phi} \right] + \frac{L_3}{G_s J} \frac{\Phi - \varphi}{\Phi} \Psi \Big\}, \quad \Psi \leq \varphi \leq \Phi$
(4)	$\frac{R_0 R}{\bar{R}} P \left\{ \frac{\mu_2}{\alpha} \frac{\sinh \alpha (\Phi - \Psi)}{\sinh \alpha \Phi} \sinh \alpha \varphi + \alpha^2 \left[\mu_2 - \frac{\bar{R}^2}{G_s J (\alpha^2 + 1)} \right] \frac{\sin (\Phi - \Psi)}{\sin \Phi} \sin \varphi \right.$ $- \mu_1 \left[\frac{\sin (\Phi - \Psi)}{\sin \Phi} \left(\Phi \cos \Phi \frac{\sin \varphi}{\sin \Phi} - \varphi \cos \varphi \right) \right.$ $\left. + (\sin \overline{\Phi - \varphi} - \overline{\Phi - \varphi} \cos \overline{\Phi - \varphi}) \frac{\sin \varphi}{\sin \Phi} + \frac{R_0 \bar{R}}{G_s J} \frac{\Phi - \Psi}{\Phi} \varphi \right\}, \quad 0 \leq \varphi \leq \Psi$ $\frac{R_0 R}{\bar{R}} P \left\{ \frac{\mu_2}{\alpha} \frac{\sinh \alpha (\Phi - \varphi)}{\sinh \alpha \Phi} \sinh \alpha \Psi + \alpha^2 \left[\mu_2 - \frac{\bar{R}^2}{G_s J (\alpha^2 + 1)} \right] \frac{\sin (\Phi - \varphi)}{\sin \Phi} \sin \Psi \right.$ $- \mu_1 \left[\frac{\sin (\Phi - \varphi)}{\sin \Phi} \left(\Phi \cos \Phi \frac{\sin \Psi}{\sin \Phi} - \Psi \cos \Psi \right) \right.$ $\left. + (\sin \overline{\Phi - \varphi} - \overline{\Phi - \varphi} \cos \overline{\Phi - \varphi}) \frac{\sin \Psi}{\sin \Phi} \right] + \frac{R_0 \bar{R}}{G_s J} \frac{\Phi - \varphi}{\Phi} \Psi \Big\}, \quad \Psi \leq \varphi \leq \Phi$

(5)	$ \begin{aligned} & R_0 R p_0 \left\{ \frac{\kappa_2}{\alpha^2} \frac{\cosh \alpha (\Phi - \Psi) - 1}{\sinh \alpha \Phi} \sinh \alpha \varphi - \omega_1 \frac{1 - \cos (\Phi - \Psi)}{\sin \Phi} \sin \varphi \right. \\ & \quad + \frac{L_2 \varphi}{2 G_s J \Phi} (\Phi - \Psi)^2 - \kappa_1 \left[\frac{1 - \cos (\Phi - \Psi)}{\sin \Phi} \left(\Phi \cos \Phi \frac{\sin \varphi}{\sin \Phi} - \varphi \cos \varphi \right) \right. \\ & \quad \left. \left. - (\Phi - \Psi) \sin (\Phi - \Psi) \frac{\sin \varphi}{\sin \Phi} \right] \right\}, \quad 0 \leq \varphi \leq \Psi \\ & R_0 R p_0 \left\{ - \frac{\kappa_2}{\alpha^2} \frac{\sinh \alpha \varphi + \cosh \alpha \Psi \sinh \alpha (\Phi - \varphi)}{\sinh \alpha \Phi} - \omega_1 \frac{\sin \varphi + \cos \Psi \sin (\Phi - \varphi)}{\sin \Phi} \right. \\ & \quad + \frac{1}{G_s J} \left[L_1 + L_2 \left(\frac{\varphi}{2 \Phi} \overline{\Phi - \Psi}^2 - \frac{1}{2} \overline{\varphi - \Psi}^2 - \frac{1}{\alpha^2} \right) \right] - \frac{\kappa_1}{\sin \Phi} \left[(\cos \Phi - \cos \Psi) \frac{\Phi \sin \varphi}{\sin \Phi} \right. \\ & \quad \left. \left. - \varphi \cos \varphi + \varphi \cos (\Phi - \varphi) \cos \Psi + \Psi \sin (\Phi - \varphi) \sin \Psi \right] + \kappa_3 \right\}, \quad \Psi \leq \varphi \leq \Phi \end{aligned} $
(6)	$ \begin{aligned} & -m_T R_0 R \left\{ \frac{R^2}{E_s C_w (\alpha^2 + 1)^2 \alpha} \frac{\sinh \alpha (\Phi - \Psi)}{\sinh \alpha \Phi} \sinh \alpha \varphi \right. \\ & \quad + \frac{\alpha^2}{\alpha^2 + 1} \left[\frac{R^2}{E_s C_w (\alpha^2 + 1)} - \frac{1}{G_s J} \right] \frac{\sin (\Phi - \Psi)}{\sin \Phi} \sin \varphi \\ & \quad - \frac{\lambda}{R^2} \left[\frac{\sin (\Phi - \Psi)}{\sin \Phi} \left(\Phi \cos \Phi \frac{\sin \varphi}{\sin \Phi} - \varphi \cos \varphi \right) \right. \\ & \quad \left. \left. + (\sin \Phi - \Psi - \Phi - \Psi \cos \Phi - \Psi) \frac{\sin \varphi}{\sin \Phi} \right] \right\}, \quad 0 \leq \varphi \leq \Psi \\ & -m_T R_0 R \left\{ \frac{R^2}{E_s C_w (\alpha^2 + 1)^2 \alpha} \frac{\sinh \alpha (\Phi - \varphi)}{\sinh \alpha \Phi} \sinh \alpha \Psi \right. \\ & \quad + \frac{\alpha^2}{\alpha^2 + 1} \left[\frac{R^2}{E_s C_w (\alpha^2 + 1)} - \frac{1}{G_s J} \right] \frac{\sin (\Phi - \varphi)}{\sin \Phi} \sin \Psi \\ & \quad - \frac{\lambda}{R^2} \left[\frac{\sin (\Phi - \varphi)}{\sin \Phi} \left(\Phi \cos \Phi \frac{\sin \Psi}{\sin \Phi} - \Psi \cos \Psi \right) \right. \\ & \quad \left. \left. + (\sin \Phi - \varphi - \Phi - \varphi \cos \Phi - \varphi) \frac{\sin \Psi}{\sin \Phi} \right] \right\}, \quad \Psi \leq \varphi \leq \Phi \end{aligned} $

f) *St-Venant's Torsional Moment T_s*

St-Venant's torsional moments T_s can be easily obtained by differentiating the corresponding solutions for θ .

$$T_s = G_s J \frac{d\theta}{R d\varphi}.$$

The results are shown in Table 6.

g) *Secondary Torsional Moments T_w*

The secondary torsional moments T_w can also be calculated by

$$T_w = -E_s C_w \frac{d^3 \theta}{R^3 d\varphi^3}.$$

The solutions for T_w are shown in Table 7.

Table 6. Solutions for St-Venant's torsional moments T_s

(1)	$p_0 \left\{ \left(\frac{L_1}{\alpha^2 + 1} - \frac{L_2}{\alpha^2} \right) \alpha \frac{\cosh \alpha (\Phi - \varphi) - \cosh \alpha \varphi}{\sinh \alpha \Phi} \right. \\ \left. + \frac{L_1 \alpha^2}{\alpha^2 + 1} \frac{\cos (\Phi - \varphi) - \cos \varphi}{\sin \Phi} + L_2 \left(\frac{\Phi}{2} - \varphi \right) \right\}$
(2)	$W \left\{ \left(\frac{\bar{R}^2}{\alpha^2 + 1} - \frac{\bar{R} R_0}{\alpha^2} \right) \alpha \frac{\cosh \alpha (\Phi - \varphi) - \cosh \alpha \varphi}{\sinh \alpha \Phi} \right. \\ \left. + \frac{\bar{R}^2 \alpha^2}{\alpha^2 + 1} \frac{\cos (\Phi - \varphi) - \cos \varphi}{\sin \Phi} + \bar{R} R_0 \left(\frac{\Phi}{2} - \varphi \right) \right\}$
(3)	$\frac{W}{R_0} \left\{ \left(\frac{L_2}{\alpha^2 + 1} - \frac{L_3}{\alpha^2} \right) \alpha^2 \frac{\sinh \alpha (\Phi - \Psi)}{\sinh \alpha \Phi} \cosh \alpha \varphi \right. \\ \left. - \frac{L_2 \alpha^2}{\alpha^2 + 1} \frac{\sin (\Phi - \Psi)}{\sin \Phi} \cos \varphi + L_3 \frac{\Phi - \Psi}{\Phi} \right\}, \quad 0 \leq \varphi \leq \Psi$ $\frac{W}{R_0} \left\{ \left(\frac{L_3}{\alpha^2} - \frac{L_2}{\alpha^2 + 1} \right) \alpha^2 \frac{\cosh \alpha (\Phi - \varphi)}{\sinh \alpha \Phi} \sinh \alpha \Psi \right. \\ \left. + \frac{L_2 \alpha^2}{\alpha^2 + 1} \frac{\cos (\Phi - \varphi)}{\sin \Phi} \sin \Psi - L_3 \frac{\Psi}{\Phi} \right\}, \quad \Psi \leq \varphi \leq \Phi$
(4)	$P \left\{ \left(\frac{\bar{R}}{\alpha^2 + 1} - \frac{R_0}{\alpha^2} \right) \alpha^2 \frac{\sinh \alpha (\Phi - \Psi)}{\sinh \alpha \Phi} \cosh \alpha \varphi \right. \\ \left. - \frac{\bar{R} \alpha^2}{\alpha^2 + 1} \frac{\sin (\Phi - \Psi)}{\sin \Phi} \cos \varphi + R_0 \frac{\Phi - \Psi}{\Phi} \right\}, \quad 0 \leq \varphi \leq \Psi$ $P \left\{ \left(\frac{R_0}{\alpha^2} - \frac{\bar{R}}{\alpha^2 + 1} \right) \alpha^2 \frac{\cosh \alpha (\Phi - \varphi)}{\sinh \alpha \Phi} \sinh \alpha \Psi \right. \\ \left. + \frac{\bar{R} \alpha^2}{\alpha^2 + 1} \frac{\cos (\Phi - \varphi)}{\sin \Phi} \sin \Psi - R_0 \frac{\Psi}{\Phi} \right\}, \quad \Psi \leq \varphi \leq \Phi$
(5)	$p_0 \left\{ \left(\frac{L_1}{\alpha^2 + 1} - \frac{L_2}{\alpha^2} \right) \alpha \frac{\cosh \alpha \varphi}{\sinh \alpha \Phi} [\cosh \alpha (\Phi - \Psi) - 1] \right. \\ \left. - \frac{L_1 \alpha^2}{\alpha^2 + 1} [1 - \cos (\Phi - \Psi)] \frac{\cos \varphi}{\sin \Phi} + \frac{L_2}{2 \Phi} (\Phi - \Psi)^2 \right\}, \quad 0 \leq \varphi \leq \Psi$ $p_0 \left\{ \left(\frac{L_1}{\alpha^2 + 1} - \frac{L_2}{\alpha^2} \right) \alpha \frac{\cosh \alpha (\Phi - \varphi) \cosh \alpha \Psi - \cosh \alpha \varphi}{\sinh \alpha \Phi} \right. \\ \left. + \frac{L_1 \alpha^2}{\alpha^2 + 1} \frac{\cos (\Phi - \varphi) \cos \Psi - \cos \varphi}{\sin \Phi} + L_2 \left[\Psi - \varphi + \frac{1}{2 \Phi} (\Phi - \Psi)^2 \right] \right\}, \quad \Psi \leq \varphi \leq \Phi$
(6)	$-m_T \frac{\alpha^2}{\alpha^2 + 1} \left[\frac{\sinh \alpha (\Phi - \Psi)}{\sinh \alpha \Phi} \cosh \alpha \varphi - \frac{\sin (\Phi - \Psi)}{\sin \Phi} \cos \varphi \right], \quad 0 \leq \varphi \leq \Psi$ $m_T \frac{\alpha^2}{\alpha^2 + 1} \left[\frac{\sinh \alpha \Psi}{\sinh \alpha \Phi} \cosh \alpha (\Phi - \varphi) - \frac{\sin \Psi}{\sin \Phi} \cos (\Phi - \varphi) \right], \quad \Psi \leq \varphi \leq \Phi$

Table 7. Solutions for the secondary torsional moments T_w

(1)	$p_0 \left\{ \left(\frac{L_2}{\alpha^2} - \frac{L_1}{\alpha^2 + 1} \right) \alpha \frac{\cosh \alpha (\Phi - \varphi) - \cosh \alpha \varphi}{\sinh \alpha \Phi} + \frac{L_1}{\alpha^2 + 1} \frac{\cos (\Phi - \varphi) - \cos \varphi}{\sin \Phi} \right\}$
(2)	$W \left\{ \left(\frac{\bar{R} R_0}{\alpha^2} - \frac{\bar{R}^2}{\alpha^2 + 1} \right) \alpha \frac{\cosh \alpha (\Phi - \varphi) - \cosh \alpha \varphi}{\sinh \alpha \Phi} + \frac{\bar{R}^2}{\alpha^2 + 1} \frac{\cos (\Phi - \varphi) - \cos \varphi}{\sin \Phi} \right\}$
(3)	$\frac{W}{R_0} \left\{ \left(\frac{L_3}{\alpha^2} - \frac{L_2}{\alpha^2 + 1} \right) \alpha^2 \frac{\sinh \alpha (\Phi - \Psi)}{\sinh \alpha \Phi} \cosh \alpha \varphi - \frac{L_2}{\alpha^2 + 1} \frac{\sin (\Phi - \Psi)}{\sin \Phi} \cos \varphi \right\}, \quad 0 \leq \varphi \leq \Psi$ $\frac{W}{R_0} \left\{ \left(\frac{L_2}{\alpha^2 + 1} - \frac{L_3}{\alpha^2} \right) \alpha^2 \frac{\cosh \alpha (\Phi - \varphi)}{\sinh \alpha \Phi} \sinh \alpha \Psi + \frac{L_2}{\alpha^2 + 1} \frac{\cos (\Phi - \varphi)}{\sin \Phi} \sin \Psi \right\}, \quad \Psi \leq \varphi \leq \Phi$
(4)	$P \left\{ \left(\frac{R_0}{\alpha^2} - \frac{\bar{R}}{\alpha^2 + 1} \right) \alpha^2 \frac{\sinh \alpha (\Phi - \Psi)}{\sinh \alpha \Phi} \cosh \alpha \varphi - \frac{\bar{R}}{\alpha^2 + 1} \frac{\sin (\Phi - \Psi)}{\sin \Phi} \cos \varphi \right\}, \quad 0 \leq \varphi \leq \Psi$ $P \left\{ \left(\frac{\bar{R}}{\alpha^2 + 1} - \frac{R_0}{\alpha^2} \right) \alpha^2 \frac{\cosh \alpha (\Phi - \varphi)}{\sinh \alpha \Phi} \sinh \alpha \Psi + \frac{\bar{R}}{\alpha^2 + 1} \frac{\cos (\Phi - \varphi)}{\sin \Phi} \sin \Psi \right\}, \quad \Psi \leq \varphi \leq \Phi$
(5)	$p_0 \left\{ \left(\frac{L_2}{\alpha^2} - \frac{L_1}{\alpha^2 + 1} \right) \alpha \frac{\cosh \alpha (\Phi - \Psi) - 1}{\sinh \alpha \Phi} \cosh \alpha \varphi - \frac{L_1}{\alpha^2 + 1} \frac{1 - \cos (\Phi - \Psi)}{\sin \Phi} \cos \varphi \right\}, \quad 0 \leq \varphi \leq \Psi$ $p_0 \left\{ \left(\frac{L_1}{\alpha^2 + 1} - \frac{L_2}{\alpha^2} \right) \alpha \frac{\cosh \alpha \varphi - \cosh \alpha (\Phi - \varphi) \cosh \alpha \Psi}{\sinh \alpha \Phi} - \frac{L_1}{\alpha^2 + 1} \frac{\cos \varphi - \cos (\Phi - \varphi) \cos \Psi}{\sin \Phi} \right\}, \quad \Psi \leq \varphi \leq \Phi$
(6)	$\frac{m_T}{\alpha^2 + 1} \left\{ \alpha^2 \frac{\sinh \alpha (\Phi - \Psi)}{\sinh \alpha \Phi} \cosh \alpha \varphi + \frac{\sin (\Phi - \Psi)}{\sin \Phi} \cos \varphi \right\}, \quad 0 \leq \varphi \leq \Psi$ $\frac{-m_T}{\alpha^2 + 1} \left\{ \alpha^2 \frac{\sinh \alpha \Psi}{\sinh \alpha \Phi} \cosh \alpha (\Phi - \varphi) + \frac{\sin \Psi}{\sin \Phi} \cos (\Phi - \varphi) \right\}, \quad \Psi \leq \varphi \leq \Phi$

h) Total Torsional Moments T

The total torsional moments T can be calculated from the formula, $T = T_s + T_w$ and shown in Table 8.

i) Shearing Forces Q

By using the Eq. (5), shearing force Q can be obtained from the solutions M_y and T found in Table 1 and 8.

$$Q = \frac{1}{R_0} \left(\frac{dM_y}{d\varphi} + T \right). \quad (5')$$

The results is shown in Table 9. It is evident on viewing the Eq. (5)' that the torsion contributes to the shearing force in the curved girder bridge.

Table 8. Solutions for total torsional moments T

(1)	$p_0 \left\{ L_1 \frac{\cos(\Phi - \varphi) - \cos \varphi}{\sin \Phi} + L_2 \left(\frac{\Phi}{2} - \varphi \right) \right\}$
(2)	$\bar{R} W \left\{ \bar{R} \frac{\cos(\Phi - \varphi) - \cos \varphi}{\sin \Phi} + R_0 \left(\frac{\Phi}{2} - \varphi \right) \right\}$
(3)	$-\frac{W}{R_0} \left\{ L_2 \frac{\sin(\Phi - \Psi)}{\sin \Phi} \cos \varphi - L_3 \frac{\Phi - \Psi}{\Phi} \right\}, \quad 0 \leq \varphi \leq \Psi$ $\frac{W}{R_0} \left\{ L_2 \frac{\cos(\Phi - \varphi)}{\sin \Phi} \sin \Psi - L_3 \frac{\Psi}{\Phi} \right\}, \quad \Psi \leq \varphi \leq \Phi$
(4)	$-P \left\{ \bar{R} \frac{\sin(\Phi - \Psi)}{\sin \Phi} \cos \varphi - R_0 \frac{\Phi - \Psi}{\Phi} \right\}, \quad 0 \leq \varphi \leq \Psi$ $P \left\{ \bar{R} \frac{\cos(\Phi - \varphi)}{\sin \Phi} \sin \Psi - R_0 \frac{\Psi}{\Phi} \right\}, \quad \Psi \leq \varphi \leq \Phi$
(5)	$p_0 \left\{ -L_1 \frac{1 - \cos(\Phi - \Psi)}{\sin \Phi} \cos \varphi + \frac{L_2}{2\Phi} (\Phi - \Psi)^2 \right\}, \quad 0 \leq \varphi \leq \Psi$ $p_0 \left\{ L_1 \frac{\cos(\Phi - \varphi) \cos \Psi - \cos \varphi}{\sin \Phi} + L_2 \left(\frac{\Phi^2 + \Psi^2}{2\Phi} - \varphi \right) \right\}, \quad \Psi \leq \varphi \leq \Phi$
(6)	$m_T \frac{\sin(\Phi - \Psi)}{\sin \Phi} \cos \varphi, \quad 0 \leq \varphi \leq \Psi$ $-m_T \frac{\sin \Psi}{\sin \Phi} \cos(\Phi - \varphi), \quad \Psi \leq \varphi \leq \Phi$

3. Stress Formulae

The stress at any point in the curved girder bridge may be easily calculated by using the solutions for various stress resultants given in preceding section. For practical purpose, the following stress formulae are very important.

a) Normal Stress σ

$$\sigma = \frac{N}{F_s} \frac{R}{n \rho} + \left(\frac{M_z I_y - M_y I_{yz}}{I_y I_z - I_{yz}^2} y + \frac{M_y I_z - M_z I_{yz}}{I_y I_z - I_{yz}^2} z \right) \frac{R}{n \rho} + \frac{M_w}{C_w} \frac{W_s}{n}. \quad (21)$$

b) Shearing Stress τ

For the shearing stress, either of two different expressions should be used according to the situation of the considering point, that is to say:

I. At any point in nonboundary wall surrounding the k th. cell,

$$\tau = -(H \check{q}_h + \bar{Q} \check{q}_b) \frac{1}{t} + \frac{R^2}{\rho^2} \frac{\check{q}_k}{t} \frac{T_s}{J} + \frac{q^*}{t} \frac{T_w}{C_w}. \quad (22-1)$$

Table 9. Solution of shearing force Q

(1)	$\frac{L_2}{R_0} p_0 \left(\frac{\Phi}{2} - \varphi \right)$
(2)	$\bar{R} W \left(\frac{\Phi}{2} - \varphi \right)$
(3)	$(\bar{R}_a - \bar{R}_i) W \frac{\Phi - \Psi}{\Phi}, \quad 0 \leq \varphi \leq \Psi$ $-(\bar{R}_a - \bar{R}_i) W \frac{\Psi}{\Phi}, \quad \Psi \leq \varphi \leq \Phi$
(4)	$P \frac{\Phi - \Psi}{\Phi}, \quad 0 \leq \varphi \leq \Psi$ $-P \frac{\Psi}{\Phi}, \quad \Psi \leq \varphi \leq \Phi$
(5)	$\frac{p_0}{4\Phi} (\bar{R}_a^2 - \bar{R}_i^2) (\Phi - \Psi)^2, \quad 0 \leq \varphi \leq \Psi$ $\frac{p_0}{2} (\bar{R}_a^2 - \bar{R}_i^2) \left(\frac{\Phi^2 + \Psi^2}{2\Phi} - \varphi \right), \quad \Psi \leq \varphi \leq \Phi$
(6)	0

II. At any point in boundary wall between the k th. and $k \pm 1$ th. cell,

$$\tau = -(H \check{q}_h + \bar{Q} \check{q}_b) \frac{1}{t} + \frac{R^2}{\rho^2} (\check{q}_k - \check{q}_{k \pm 1}) \frac{T_s}{tJ} + \frac{q^*}{t} \frac{T_w}{C_w}. \quad (22-2)$$

The quantity \bar{Q} included in the formula (22) represents the shearing force due to bending and its corresponding values to the above mentioned typical loading conditions are given in Table 10.

4. Strain Energy Stored in Continuous Curved Girder Bridge

Under the general loading condition, the strain energy Π stored in continuous curved girder bridge may be expressed as a following formula.

$$\Pi = \sum_m \frac{1}{2} \int_0^{\Phi_m} \int_{F_m} \left(\frac{\sigma^2}{E} + \frac{\tau^2}{G} \right) \rho_m dF_m d\varphi_m, \quad (23)$$

where \sum_m means the total of the strain energy all over the length of continuous curved girder bridge. And also suffix m denotes the quantity concerned with the m th. span.

Table 10. Shear forces due to bending \bar{Q}

(1)	$p_0 L_1 \frac{\cos \varphi - \cos (\Phi - \varphi)}{\sin \Phi} \frac{1}{R_0}$
(2)	$W \bar{R}^2 \frac{\cos \varphi - \cos (\Phi - \varphi)}{\sin \Phi} \frac{1}{R_0}$
(3)	$W \frac{L_2}{R_0} \frac{\sin (\Phi - \Psi)}{\sin \Phi} \cos \varphi \frac{1}{R_0}, \quad 0 \leq \varphi \leq \Psi$ $- W \frac{L_2}{R_0} \frac{\cos (\Phi - \varphi)}{\sin \Phi} \sin \Psi \frac{1}{R_0}, \quad \Psi \leq \varphi \leq \Phi$
(4)	$P \bar{R} \frac{\sin (\Phi - \Psi)}{\sin \Phi} \cos \varphi \frac{1}{R_0}, \quad 0 \leq \varphi \leq \Psi$ $- P \bar{R} \frac{\cos (\Phi - \varphi)}{\sin \Phi} \sin \Psi \frac{1}{R_0}, \quad \Psi \leq \varphi \leq \Phi$
(5)	$p_0 L_1 \frac{1 - \cos (\Phi - \Psi)}{\sin \Phi} \cos \varphi \frac{1}{R_0}, \quad 0 \leq \varphi \leq \Psi$ $p_0 L_1 \frac{\cos \varphi - \cos (\Phi - \varphi) \cos \Psi}{\sin \Phi} \frac{1}{R_0}, \quad \Psi \leq \varphi \leq \Phi$
(6)	$- m_T \frac{\sin (\Phi - \Psi)}{\sin \Phi} \cos \varphi \frac{1}{R_0}, \quad 0 \leq \varphi \leq \Psi$ $m_T \frac{\cos (\Phi - \varphi)}{\sin \Phi} \sin \Psi \frac{1}{R_0}, \quad \Psi \leq \varphi \leq \Phi$

Substituting the stress formula [formula (21) and (22) in previous section 3] into expression (23), and arranging that, a following simplified expression may be obtained.

$$\Pi = \sum_m \frac{R_m}{2} \int_0^{\Phi_m} \left\{ \frac{1}{E_s} \left(\frac{M_{ym}^2}{I'_{ym}} + \frac{M_{wm}^2}{C_{wm}} \right) + \frac{1}{G_s} \left(\frac{T_{sm}^2}{J_m} + \frac{\bar{Q}_m^2}{\underline{F'_{sm}}} + \frac{Z_m}{\underline{C_{wm}^2}} T_{wm}^2 \right) \right\} d\varphi_m, \quad (24)$$

where

$$Z = \int_F q^{*2} \frac{n_g}{t} \frac{\rho}{R} ds, \quad (25)$$

$$\frac{1}{\underline{F'_s}} = \int_F \bar{q}_b^2 \frac{n_g}{t} \frac{\rho^3}{R^3} ds. \quad (26)$$

The underlined terms may be generally neglected as compared with other terms.

5. Stress Resultants in Continuous Curved Girder Bridge

Now, by cutting a prescribed continuous curved girder bridge at the cross sections on every intermediate supports, the simply supported girder system

will be produced. So, they have a couple of bending moment and warping moment at both ends of each span.

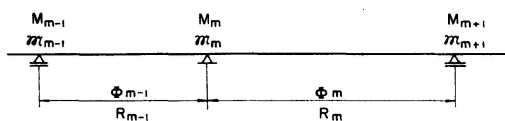


Fig. 3. Continuous curved girder bridge.

The stress resultants which will be caused at the bridge section defined by peripheral coordinate φ_m may be readily given by the following formulae, where the quantities with suffix 0 represent the stress resultants of the imaginary simply supported curved girder bridge in the m th. span under given loading. $\varphi'_m = \Phi_m - \varphi_m$.

a) Bending Moment M_{ym}

$$M_{ym} = M_{m0} + M_m \frac{\sin \varphi'_m}{\sin \Phi_m} + M_{m+1} \frac{\sin \varphi_m}{\sin \Phi_m}. \quad (27)$$

b) Warping Moment M_{wm}

$$M_{wm} = M_{wm0} + \mathfrak{M}_m \frac{\sinh \alpha_m \varphi'_m}{\sinh \alpha_m \Phi_m} + \mathfrak{M}_{m+1} \frac{\sinh \alpha_m \varphi_m}{\sinh \alpha_m \Phi_m} \\ + \frac{R_m}{\alpha_m^2 + 1} \left\{ M_m \left[\frac{\sin \varphi'_m}{\sin \Phi_m} - \frac{\sinh \alpha_m \varphi'_m}{\sinh \alpha_m \Phi_m} \right] + M_{m+1} \left[\frac{\sin \varphi_m}{\sin \Phi_m} - \frac{\sinh \alpha_m \varphi_m}{\sinh \alpha_m \Phi_m} \right] \right\}. \quad (28)$$

c) St-Venant's Torsional Moment T_{sm}

$$T_{sm} = T_{sm0} + \frac{\mathfrak{M}_m}{R_m} \left(\frac{1}{\Phi_m} - \frac{\alpha_m \cosh \alpha_m \varphi'_m}{\sinh \alpha_m \Phi_m} \right) + \frac{\mathfrak{M}_{m+1}}{R_m} \left(\frac{\alpha_m \cosh \alpha_m \varphi_m}{\sinh \alpha_m \Phi_m} - \frac{1}{\Phi_m} \right) \\ + M_m \left[\frac{1}{\alpha_m^2 + 1} \left(\alpha_m^2 \frac{\cos \varphi'_m}{\sin \Phi_m} + \alpha_m \frac{\cosh \alpha_m \varphi'_m}{\sinh \alpha_m \Phi_m} \right) - \frac{1}{\Phi_m} \right] \\ + M_{m+1} \left[\frac{1}{\Phi_m} - \frac{1}{\alpha_m^2 + 1} \left(\alpha_m^2 \frac{\cos \varphi_m}{\sin \Phi_m} + \alpha_m \frac{\cosh \alpha_m \varphi_m}{\sinh \alpha_m \Phi_m} \right) \right]. \quad (29)$$

d) Secondary Torsional Moment T_{wm}

$$T_{wm} = T_{wm0} + \frac{1}{R_m} \left(\mathfrak{M}_m \frac{\alpha_m \cosh \alpha_m \varphi'_m}{\sinh \alpha_m \Phi_m} - \mathfrak{M}_{m+1} \frac{\alpha_m \cosh \alpha_m \varphi_m}{\sinh \alpha_m \Phi_m} \right) \\ + \frac{1}{\alpha_m^2 + 1} \left[M_m \left(\frac{\cos \varphi'_m}{\sin \Phi_m} - \frac{\alpha_m \cosh \alpha_m \varphi'_m}{\sinh \alpha_m \Phi_m} \right) - M_{m+1} \left(\frac{\cos \varphi_m}{\sin \Phi_m} - \frac{\alpha_m \cosh \alpha_m \varphi_m}{\sinh \alpha_m \Phi_m} \right) \right]. \quad (30)$$

e) Shearing Force due to Bending \bar{Q}_m

$$\bar{Q}_m = \bar{Q}_{m0} - \frac{1}{R_{0m}} \left(M_m \frac{\cos \varphi'_m}{\sin \Phi_m} - M_{m+1} \frac{\cos \varphi_m}{\sin \Phi_m} \right). \quad (31)$$

f) Total Torsional Moment T_m

$$T_m = T_{m0} + \frac{1}{l_m} (\mathfrak{M}_m - \mathfrak{M}_{m+1}) + M_m \left(\frac{\cos \varphi'_m}{\sin \Phi_m} - \frac{1}{\Phi_m} \right) + M_{m+1} \left(\frac{1}{\Phi_m} - \frac{\cos \varphi_m}{\sin \Phi_m} \right). \quad (32)$$

6. Elastic Equations for Continuous Curved Girder Bridge

In order to find both unknown end moments M_m and \mathfrak{M}_m , principle of least work may be applied to the whole system composed of main girders.

$$\frac{\partial \Pi}{\partial M_m} = 0, \quad \frac{\partial \Pi}{\partial \mathfrak{M}_m} = 0.$$

Substituting expression (24) into above conditions, and then using the stress resultants (27) to (31), a set of simultaneous equations for unknown quantities M_m and \mathfrak{M}_m .

$$\begin{aligned} a_{m,m-1} M_{m-1} + a_{mm} M_m + a_{m,m+1} M_{m+1} + b_{m,m-1} \mathfrak{M}_{m-1} \\ + b_{mm} \mathfrak{M}_m + b_{m,m+1} \mathfrak{M}_{m+1} = -L_m, \\ b_{m,m-1} M_{m-1} + b_{mm} M_m + b_{m,m+1} M_{m+1} + d_{m,m-1} \mathfrak{M}_{m-1} \\ + d_{mm} \mathfrak{M}_m + d_{m,m+1} \mathfrak{M}_{m+1} = -N_m, \\ (m = 1, 2, \dots, n-1). \end{aligned} \quad (33)$$

If the structure is simply supported at both ends ($m=0$, and $m=n$), $M_0 = M_n = 0$, $\mathfrak{M}_0 = \mathfrak{M}_n = 0$.

Coefficients a , b , and d contained in Eqs. (33) may be given by the following expression.

$$a_{mm} = \sum_{j=m-1}^m [a]_{mj} \quad (34)$$

and

$$\begin{aligned} [a]_{mj} = \frac{R_j}{2 E_s I'_{yj}} \left[\frac{\Phi_j - \sin \Phi_j \cos \Phi_j}{\sin^2 \Phi_j} \right] + \frac{R_j}{G_s J_j} \left[\frac{\alpha_j^2}{2(\alpha_j^2 + 1)} \frac{\Phi_j + \sin \Phi_j \cos \Phi_j}{\sin^2 \Phi_j} \right. \\ \left. + \frac{\alpha_j^2}{(\alpha_j^2 + 1)^2} \left(\frac{\cos \Phi_j}{\sin \Phi_j} + \frac{\cosh \alpha_j \Phi_j}{\alpha_j \sinh \alpha_j \Phi_j} \right) - \frac{1}{\Phi_j} \right], \end{aligned} \quad (35)$$

$$\begin{aligned} a_{m,m+1} = \frac{R_m}{2 E_s I'_{ym}} \left[\frac{\sin \Phi_m - \Phi_m \cos \Phi_m}{\sin^2 \Phi_m} \right] - \frac{R_m}{G_s J_m} \left[\frac{\alpha_m^2}{2(\alpha_m^2 + 1)} \frac{\sin \Phi_m + \Phi_m \cos \Phi_m}{\sin^2 \Phi_m} \right. \\ \left. + \frac{\alpha_m^2}{(\alpha_m^2 + 1)^2} \left(\frac{1}{\sin \Phi_m} + \frac{1}{\alpha_m \sinh \alpha_m \Phi_m} \right) - \frac{1}{\Phi_m} \right], \end{aligned} \quad (36)$$

$$\begin{aligned} a_{m,m-1} = \frac{R_{m-1}}{2 E_s I'_{y,m-1}} \left[\frac{\sin \Phi_{m-1} - \Phi_{m-1} \cos \Phi_{m-1}}{\sin^2 \Phi_{m-1}} \right] \\ - \frac{R_{m-1}}{G_s J_{m-1}} \left[\frac{\alpha_{m-1}^2}{2(\alpha_{m-1}^2 + 1)} \frac{\sin \Phi_{m-1} + \Phi_{m-1} \cos \Phi_{m-1}}{\sin^2 \Phi_{m-1}} \right. \\ \left. + \frac{\alpha_{m-1}^2}{(\alpha_{m-1}^2 + 1)^2} \left(\frac{1}{\sin \Phi_{m-1}} + \frac{1}{\alpha_{m-1} \sinh \alpha_{m-1} \Phi_{m-1}} \right) - \frac{1}{\Phi_{m-1}} \right], \end{aligned} \quad (37)$$

$$b_{mm} = \sum_{j=m-1}^m [b]_{mj}, \quad (38)$$

$$[b]_{mj} = \frac{1}{G_s J_j} \left[\frac{1}{\Phi_j} - \frac{\alpha_j^2}{\alpha_j^2 + 1} \left(\alpha_j \frac{\cos \Phi_j}{\sin \Phi_j} + \frac{\cosh \alpha_j \Phi_j}{\sinh \alpha_j \Phi_j} \right) \right], \quad (39)$$

$$b_{m,m+1} = \frac{1}{G_s J_m} \left[\frac{\alpha_m}{\alpha_m^2 + 1} \left(\alpha_m \frac{1}{\sin \Phi_m} + \frac{1}{\sinh \alpha_m \Phi_m} \right) - \frac{1}{\Phi_m} \right], \quad (40)$$

$$b_{m,m-1} = \frac{1}{G_s J_{m-1}} \left[\frac{\alpha_{m-1}}{\alpha_{m-1}^2 + 1} \left(\alpha_{m-1} \frac{1}{\sin \Phi_{m-1}} + \frac{1}{\sinh \alpha_{m-1} \Phi_{m-1}} \right) - \frac{1}{\Phi_{m-1}} \right], \quad (41)$$

$$d_{mm} = \sum_{j=m-1}^m [d]_{mj}, \quad (42)$$

$$[d]_{mj} = \frac{1}{G_s J_j R_j} \left[\alpha_j \frac{\cosh \alpha_j \Phi_j}{\sinh \alpha_j \Phi_j} - \frac{1}{\Phi_j} \right], \quad (43)$$

$$d_{m,m+1} = \frac{1}{G_s J_m R_m} \left(\frac{1}{\Phi_m} - \alpha_m \frac{1}{\sinh \alpha_m \Phi_m} \right), \quad (44)$$

$$d_{m,m-1} = \frac{1}{G_s J_{m-1} R_{m-1}} \left(\frac{1}{\Phi_{m-1}} - \alpha_{m-1} \frac{1}{\sinh \alpha_{m-1} \Phi_{m-1}} \right). \quad (45)$$

From formulae (36), (37), (40), (41), (44), and (45), it may be seen that the following reciprocal relations can be satisfied.

$$a_{m \ m+1} = a_{m+1, m}, \quad b_{m, m+1} = b_{m+1, m}, \quad d_{m, m+1} = d_{m+1 \ m}.$$

7. Loading Terms of Elastic Equations

For several typical loading conditions, the loading terms contained in the right-hand side of elastic equations may be obtained as follows:

a) Uniformly distributed load

In the case when the uniformly distributed load p_j per unit area of floor slab in the j th. span, the loading terms L_{mj} and N_{mj} may be expressed as follows:

$$\begin{aligned} L_{mj} = p_j & \left[\mathfrak{L}_{1j} \frac{R_j}{E_s I'_{yj}} \frac{(1 - \cos \Phi_j)(\Phi_j - \sin \Phi_j)}{2 \sin^2 \Phi_j} \right. \\ & + \frac{R_j}{G_s J_j} \left[\mathfrak{L}_{1j} \frac{\alpha_j^2}{2(\alpha_j^2 + 1)^2} \left\{ \left(\frac{1}{\alpha_j^2 + 1} \frac{\Phi_j}{\sin \Phi_j} - \frac{1}{\alpha_j^2 + 3} \right) \tan \frac{\Phi_j}{2} + \frac{2}{\alpha_j} \tanh \frac{\alpha_j \Phi_j}{2} \right\} \right. \\ & \left. \left. - \mathfrak{L}_{2j} \left\{ \frac{1}{\alpha_j^2 + 1} \left(\alpha_j^2 \tan \frac{\Phi_j}{2} + \frac{1}{\alpha_j} \tanh \frac{\alpha_j \Phi_j}{2} \right) - \frac{\Phi_j}{2} \right\} \right] \right], \quad (46) \end{aligned}$$

$$N_{mj} = \frac{p_j}{G_s J_j} \left\{ \mathfrak{L}_{1j} \frac{\alpha_j^2}{\alpha_j^2 + 1} \left(\tan \frac{\Phi_j}{2} - \frac{1}{\alpha_j} \tanh \frac{\alpha_j \Phi_j}{2} \right) + \mathfrak{L}_{2j} \left(\frac{1}{\alpha_j} \tanh \frac{\alpha_j \Phi_j}{2} - \frac{\Phi_j}{2} \right) \right\}, \quad (47)$$

where

$$\mathfrak{L}_{1j} = \frac{1}{3} (\bar{R}_{aj}^3 - \bar{R}_{ij}^3), \quad (48)$$

$$\mathfrak{L}_{2j} = \frac{R_{0j}}{2} (\bar{R}_{aj}^2 - \bar{R}_{ij}^2). \quad (49)$$

b) Axial Line Load

If we put $\mathfrak{L}_{1j} \rightarrow \bar{R}_j^2$, $\mathfrak{L}_{2j} \rightarrow \bar{R}_j R_{0j}$, $p_j \rightarrow W_j$ in both Eqs. (46) and (47), the loading terms L_{mj} and N_{mj} for an axial line load may be obtained directly.

c) Radial Line Load

Let us consider the case of radial line load W_j per unit length. It also is assumed to be placed at the situation $\varphi_j = \psi_j$ in the j th. span.

$$\begin{aligned}
 L_{mm} = & \frac{W_m}{R_{0m}} \left[\frac{R_m}{E_s I'_{ym}} \mathfrak{L}_{2m} \frac{\psi'_m \sin \psi_m - \psi_m \sin \psi'_m \cos \Phi_m}{2 \sin^2 \Phi_m} \right. \\
 & + \frac{R_m}{G_s J_m} \left[\mathfrak{L}_{2m} \frac{\alpha_m^2}{(\alpha_m^2 + 1)^2} \left(\sqrt{\alpha_m^2 + 1} \frac{\psi'_m \sin \psi_m - \psi_m \sin \psi'_m \cos \Phi_m}{2 \sin^2 \Phi_m} \right. \right. \\
 & - \frac{\sin \psi'_m}{\sin \Phi_m} + \frac{\sinh \alpha_m \psi'_m}{\sinh \alpha_m \Phi_m} \left. \right) - \mathfrak{L}_{3m} \left(\frac{1}{\alpha_m^2 + 1} \left\{ \frac{\alpha_m^2 \sin \psi'_m}{\sin \Phi_m} \right. \right. \\
 & \left. \left. + \frac{\sinh \alpha_m \psi'_m}{\sinh \alpha_m \Phi_m} \right\} - \frac{\psi'_m}{\Phi_m} \right) \left. \right] \left. \right], \quad (50)
 \end{aligned}$$

$$\begin{aligned}
 L_{m,m-1} = & \frac{W_{m-1}}{R_{0,m-1}} \left[\frac{R_{m-1}}{E_s I'_{y,m-1}} \mathfrak{L}_{2,m-1} \frac{\psi_{m-1} \sin \psi'_{m-1} - \psi'_{m-1} \sin \psi_{m-1} \cos \Phi_{m-1}}{2 \sin^2 \Phi_{m-1}} \right. \\
 & + \frac{R_{m-1}}{G_s J_{m-1}} \left[\mathfrak{L}_{2,m-1} \frac{\alpha_{m-1}^2}{(\alpha_{m-1}^2 + 1)^2} \cdot \right. \\
 & \cdot \left(\sqrt{\alpha_{m-1}^2 + 1} \frac{\psi_{m-1} \sin \psi'_{m-1} - \psi'_{m-1} \sin \psi_{m-1} \cos \Phi_{m-1}}{2 \sin^2 \Phi_{m-1}} - \frac{\sin \psi_{m-1}}{\sin \Phi_{m-1}} \right. \\
 & + \frac{\sinh \alpha_{m-1} \psi_{m-1}}{\sinh \alpha_{m-1} \Phi_{m-1}} \left. \right) - \mathfrak{L}_{3,m-1} \left(\frac{1}{\alpha_{m-1}^2 + 1} \left\{ \frac{\alpha_{m-1}^2 \sin \psi_{m-1}}{\sin \Phi_{m-1}} \right. \right. \\
 & \left. \left. + \frac{\sinh \alpha_{m-1} \psi_{m-1}}{\sinh \alpha_{m-1} \Phi_{m-1}} \right\} - \frac{\psi_{m-1}}{\Phi_{m-1}} \right) \left. \right] \left. \right], \quad (51)
 \end{aligned}$$

$$\begin{aligned}
 N_{mm} = & \frac{W_m}{R_{0m} G_s J_m} \left\{ \mathfrak{L}_{2m} \frac{\alpha_m^2}{\alpha_m^2 + 1} \left(\frac{\sin \psi'_m}{\sin \Phi_m} - \frac{\sinh \alpha_m \psi'_m}{\sinh \alpha_m \Phi_m} \right) \right. \\
 & \left. + \mathfrak{L}_{3m} \left(\frac{\sinh \alpha_m \psi'_m}{\sinh \alpha_m \Phi_m} - \frac{\psi'_m}{\Phi_m} \right) \right\}, \quad (52)
 \end{aligned}$$

$$\begin{aligned}
 N_{m,m-1} = & \frac{W_{m-1}}{R_{0,m-1} G_s J_{m-1}} \left\{ \mathfrak{L}_{2,m-1} \frac{\alpha_{m-1}^2}{\alpha_{m-1}^2 + 1} \left(\frac{\sin \psi_{m-1}}{\sin \Phi_{m-1}} - \frac{\sinh \alpha_{m-1} \psi_{m-1}}{\sinh \alpha_{m-1} \Phi_{m-1}} \right) \right. \\
 & \left. + \mathfrak{L}_{3,m-1} \left(\frac{\sinh \alpha_{m-1} \psi_{m-1}}{\sinh \alpha_{m-1} \Phi_{m-1}} - \frac{\psi_{m-1}}{\Phi_{m-1}} \right) \right\}, \quad (53)
 \end{aligned}$$

$$\text{where} \quad \mathfrak{L}_{3m} = \bar{R}_{0m}^2 (\bar{R}_{am} - R_{im}). \quad (54)$$

d) Concentrated Load

If we put $W_j \rightarrow R_{0j} P_j$, $\mathfrak{L}_{2j} \rightarrow \bar{R}_j$, $\mathfrak{L}_{3j} \rightarrow R_{0j}$ in Eqs. (50) to (35), the loading terms L_{mj} and N_{mj} for a concentrated load P_j may be directly obtained.

It also is assumed to be placed at the situation designated by coordinates $\varphi_j = \psi_j$ and $\rho = \bar{R}_j$.

Thus, under the simultaneous loads acting on both the m th. and the $m + 1$ th. spans, the loading terms L_m and N_m may be given as follows:

$$L_m = L_{mm} + L_{m,m-1}, \quad N_m = N_{mm} + N_{m,m-1}. \quad (55)$$

8. Coefficients and Loading Terms of Elastic Equations for Straight Span

Let us consider the continuous girder bridge where the straight girders are connected with the curved ones on the intermediate supports. For the curved span, coefficients and loading terms of elastic Eqs. (33) may be evaluated again according to previous formulae as shown in sections 6 and 7. While the following formulae should be used for the straight span.

a) Coefficients of Elastic Equations

I. The Case Where the m th. Span is Straight

$$a_{mm} = \frac{l_m}{3 E_s I'_{ym}} + [a]_{m,m-1}, \quad (56)$$

$$a_{m,m+1} = \frac{l_m}{6 E_s I'_{ym}}, \quad (57)$$

$$b_{mm} = [b]_{m,m-1}, \quad b_{m,m+1} = 0,$$

$$d_{mm} = \frac{1}{G_s J_m} \left(\bar{\alpha}_m \frac{\cosh \bar{\alpha}_m l_m}{\sinh \bar{\alpha}_m l_m} - \frac{1}{l_m} \right) + [d]_{m,m-1}, \quad (58)$$

$$d_{m,m+1} = \frac{1}{G_s J_m} \left(\frac{1}{l_m} - \frac{\bar{\alpha}_m}{\sinh \bar{\alpha}_m l_m} \right), \quad (59)$$

$$\text{where} \quad \bar{\alpha}_m = \sqrt{\frac{G_s J_m}{E_s C_{wm}}}. \quad (60)$$

II. The Case Where the $m - 1$ th. Span is Straight

$$a_{mm} = \frac{l_{m-1}}{3 E_s I'_{y,m-1}} + [a]_{mm}, \quad (61)$$

$$a_{m,m-1} = \frac{l_{m-1}}{6 E_s I'_{y,m-1}}, \quad (62)$$

$$b_{mm} = [b]_{mm}, \quad b_{m,m-1} = 0,$$

$$d_{mm} = \frac{1}{G_s J_{m-1}} \left(\bar{\alpha}_{m-1} \frac{\cosh \bar{\alpha}_{m-1} l_{m-1}}{\sinh \bar{\alpha}_{m-1} l_{m-1}} - \frac{1}{l_{m-1}} \right) + [d]_{mm}, \quad (63)$$

$$d_{m,m-1} = \frac{1}{G_s J_{m-1}} \left(\frac{1}{l_{m-1}} - \frac{\bar{\alpha}_{m-1}}{\sinh \bar{\alpha}_{m-1} l_{m-1}} \right). \quad (64)$$

b) Loading Terms of Elastic Equations

I. Uniformly Distributed Load

For the case where the uniformly distributed load p_j per unit area is placed over the breadth a_j in the j th. span, the loading terms L_{mj} and N_{mj} may be given by the following expressions.

$$L_{mj} = \frac{p_j a_j l_j^3}{24 E_s I'_{yj}}, \quad (65)$$

$$N_{mj} = \frac{p_j e_j a_j}{G_s J_j} \left(\frac{1}{\bar{\alpha}_j} \tanh \frac{\bar{\alpha}_j l_j}{2} - \frac{l_j}{2} \right), \quad (66)$$

where e_j is the horizontal distance between the shear center of the bridge section and the position of resultant of load.

The suffix j should be equal to $j = m$ or $m - 1$ for the case where the m th. or the $m - 1$ th. span is straight respectively.

II. Axial Line Load

L_{mj} and N_{mj} for an axial line load W_j , per unit length, placed with eccentricity e_j may be readily obtained by putting $p_j a_j \rightarrow W_j$ in previous formulae (65) and (66).

III. Radial Line Load

Let us consider the case of a radial line load W per unit length. It also is assumed to have a breadth a and be placed at $x = c$ with eccentricity e .

1. The case where the m th. span is straight. If the m th. span is straight and above described load acts on that span, necessary loading terms may be evaluated by the following formulae.

$$L_{mm} = \frac{W_m a_m c_m}{6 E_s I'_{ym} l_m} (2 l_m - c_m) (l_m - c_m), \quad (67)$$

$$N_{mm} = \frac{W_m e_m a_m}{G_s J_m} \left(\frac{\sinh \bar{\alpha}_m c'_m}{\sinh \bar{\alpha}_m l_m} - \frac{c'_m}{l_m} \right). \quad (68)$$

2. The case where the $m - 1$ th. span is straight

$$L_{m,m-1} = \frac{W_{m-1} a_{m-1} c_{m-1}}{6 E_s I'_{y,m-1} l_{m-1}} (l_{m-1}^2 - c_{m-1}^2), \quad (69)$$

$$N_{m,m-1} = \frac{W_{m-1} e_{m-1} a_{m-1}}{G_s J_{m-1}} \left(\frac{\sinh \bar{\alpha}_{m-1} c_{m-1}}{\sinh \bar{\alpha}_{m-1} l_{m-1}} - \frac{c_{m-1}}{l_{m-1}} \right). \quad (70)$$

III. Concentrated Load

For the case where the j th. span is straight and a concentrated load P_j acts on that span, if we put $W_j a_j \rightarrow P_j$, $j = m$ or $m - 1$ in previous formulae (67) and (68) or (69) and (70), every formulae in preceding article c) are valid again.

9. Deformations of Continuous Curved Girder Bridge

The deflection and rotating angle of cross section of the continuous curved girder bridge will be obtained by superposing the deflection and angle of rotation of imaginary simply supported bridge under the prescribed loads upon those due to end moments respectively.

a) Angle of Rotation β_m

$$\begin{aligned} \beta_m = \beta_{m0} &+ \frac{R_m^2}{E_s C_{wm} (\alpha_m^2 + 1)} \left\{ \left(\mathfrak{M}_m - \frac{R_m}{\alpha_m^2 + 1} M_m \right) \left(\frac{\sinh \alpha_m \varphi'_m}{\sinh \alpha_m \Phi_m} - \frac{\sin \varphi'_m}{\sin \Phi_m} \right) \right. \\ &+ \left(\mathfrak{M}_{m+1} - \frac{R_m}{\alpha_m^2 + 1} M_{m+1} \right) \left(\frac{\sinh \alpha_m \varphi_m}{\sinh \alpha_m \Phi_m} - \frac{\sin \varphi_m}{\sin \Phi_m} \right) \Big\} \\ &+ \frac{\lambda_m}{R_m \sin \Phi_m} \left\{ M_m \left(\varphi_m \cos \varphi'_m - \Phi_m \frac{\sin \varphi_m}{\sin \Phi_m} \right) \right. \\ &\left. + M_{m+1} \left(\Phi_m \cos \Phi_m \frac{\sin \varphi_m}{\sin \Phi_m} - \varphi_m \cos \varphi_m \right) \right\}, \end{aligned} \quad (71)$$

$$\text{where} \quad \lambda = \frac{R^2}{2} \left[\frac{R^2}{E_s C_w (\alpha^2 + 1)} + \frac{1}{E_s I_y} \right]. \quad (72)$$

b) Deflection δ_m

The deflection of shear center δ_m may be evaluated by the following formula.

$$\begin{aligned} \delta_m = \delta_{m0} &+ R_{0m} \left[\frac{\mathfrak{M}_m}{G_s J_m} \left[\frac{1}{\alpha_m^2 + 1} \left(\frac{\sinh \alpha_m \varphi'_m}{\sinh \alpha_m \Phi_m} + \alpha_m^2 \frac{\sin \varphi'_m}{\sin \Phi_m} \right) - \frac{\varphi'_m}{\Phi_m} \right] \right. \\ &+ \frac{\mathfrak{M}_{m+1}}{G_s J_m} \left[\frac{1}{\alpha_m^2 + 1} \left(\frac{\sinh \alpha_m \varphi_m}{\sinh \alpha_m \Phi_m} + \alpha_m^2 \frac{\sin \varphi_m}{\sin \Phi_m} \right) - \frac{\varphi_m}{\Phi_m} \right] \\ &- M_m \left\{ \left[\frac{R_m}{G_s J_m (\alpha_m^2 + 1)^2} \left(\frac{\sinh \alpha_m \varphi'_m}{\sinh \alpha_m \Phi_m} + \sqrt{\alpha_m^2 + 2} \alpha_m^2 \frac{\sin \varphi'_m}{\sin \Phi_m} \right) - \frac{R_m}{G_s J_m} \frac{\varphi'_m}{\Phi_m} \right] \right. \\ &\left. + \frac{\lambda_m}{R_m \sin \Phi_m} \left(\varphi_m \cos \varphi'_m - \Phi_m \frac{\sin \varphi_m}{\sin \Phi_m} \right) \right\} \\ &- M_{m+1} \left\{ \left[\frac{R_m}{G_s J_m (\alpha_m^2 + 1)^2} \left(\frac{\sinh \alpha_m \varphi_m}{\sinh \alpha_m \Phi_m} + \sqrt{\alpha_m^2 + 2} \alpha_m^2 \frac{\sin \varphi_m}{\sin \Phi_m} \right) - \frac{R_m}{G_s J_m} \frac{\varphi_m}{\Phi_m} \right] \right. \\ &\left. \left. + \frac{\lambda_m}{R_m \sin \Phi_m} \left(\Phi_m \cos \Phi_m \frac{\sin \varphi_m}{\sin \Phi_m} - \varphi_m \cos \varphi_m \right) \right] \right\}. \end{aligned} \quad (73)$$

So that the deflection of a point situated at a horizontal distance Y from the shear center.

$$\delta_m(Y) = \delta_m - Y \beta_m, \quad (74)$$

where

$$Y = \rho - R_0. \quad (75)$$

10. Numerical Example

The influence of the stress resultants and deformations will be found for a three-span continuous composite box girder bridge as shown in Fig. 4a. The length of each span is equally 33.527 m. Both side spans have straight main girders while a center span has circularly curved girder with a radius of curvature 30 m. And then the road width is 6.705 m and the cross section of bridge is assumed to be constant all over the bridge length. Both the shape and main dimensions of cross section also are shown in Fig. 4b. According to

the fundamental theory developed in previous paper, the necessary cross-sectional properties have been evaluated for respective span as follows:

$$\begin{aligned}
 C_{w1} &= C_{w3} = 0.48803 \times 10^{12} \text{ cm}^6 \\
 C_{w2} &= 0.48135 \times 10^{12} \text{ cm}^6 \quad I_{y1} = I_{y3} = 10.2308 \times 10^6 \text{ cm}^4 \\
 I_{y2} &= 10.2601 \times 10^6 \text{ cm}^4 \quad J_1 = J_3 = 4.9773 \times 10^6 \text{ cm}^4 \\
 J_2 &= 5.0229 \times 10^6 \text{ cm}^4 \quad \alpha_1 = \alpha_3 = 1.972 \times 10^{-3} \text{ 1/cm} \\
 \alpha_2 &= 5.9364
 \end{aligned}$$

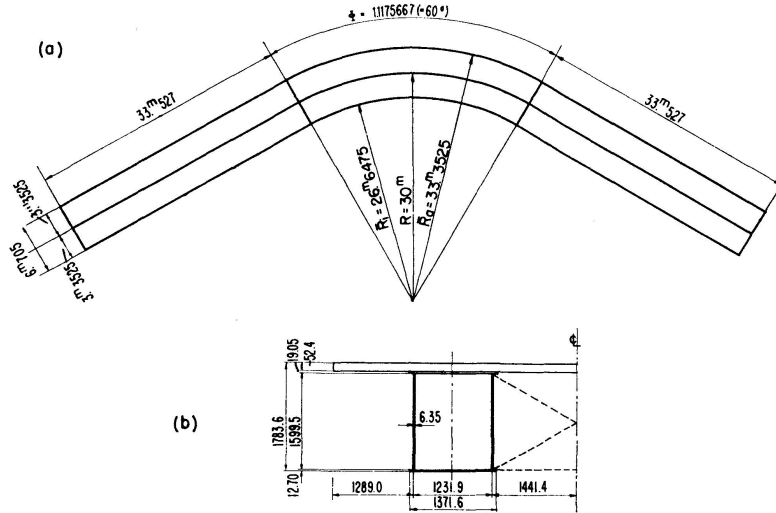


Fig. 4. Continuous curved girder bridge a), b).

The matrix representation of the elastic equations becomes as follows:

$$\begin{bmatrix}
 1.424510 & 0.561727 & 0.637130 \times 10^{-3} & 0.471472 \times 10^{-3} \\
 0.561727 & 1.424510 & 0.471472 \times 10^{-3} & 0.637130 \times 10^{-3} \\
 0.637130 \times 10^{-3} & 0.471472 \times 10^{-3} & 8.923880 \times 10^{-6} & 0.7331305 \times 10^{-6} \\
 0.471472 \times 10^{-3} & 0.637130 \times 10^{-3} & 0.7331305 \times 10^{-6} & 8.923880 \times 10^{-6}
 \end{bmatrix}
 \begin{bmatrix}
 M_2 \\
 M_3 \\
 \mathfrak{M}_2 \\
 \mathfrak{M}_3
 \end{bmatrix}
 =
 \begin{bmatrix}
 L_2 \\
 L_3 \\
 N_2 \\
 N_3
 \end{bmatrix}
 \quad (76)$$

Corresponding loading terms to respective loading condition are as follows:

I. For the Loading on the First Span:

$$L_2 = L_{21}, \quad L_3 = 0, \quad N_2 = N_{21}, \quad N_3 = 0.$$

II. For the Loading on the Second Span:

$$L_2 = L_{22}, \quad L_3 = L_{32}, \quad N_2 = N_{22}, \quad N_3 = N_{32}.$$

III. For the Loading on the Third Span:

$$L_2 = 0, \quad L_3 = L_{33}, \quad N_2 = 0, \quad N_3 = N_{33}.$$

a) *The Influence Line for Stress Resultant*

From the solutions of elastic Eq. (76), the influence lines for the bending moment M_2 and the warping moment \mathfrak{M}_2 at the intermediate supports B are given as shown in Fig. 5 and 6.

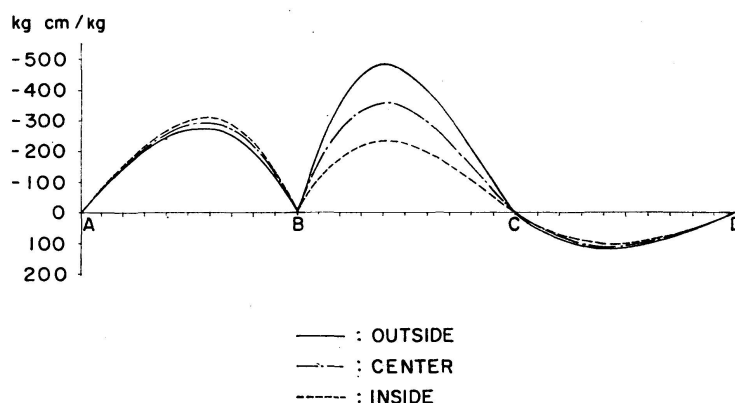


Fig. 5. The influence lines for bending moment M_2 at support B .

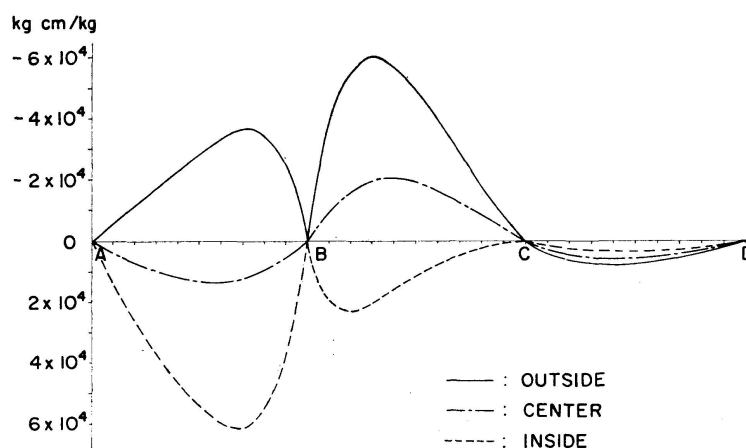


Fig. 6. The influence lines for warping moment \mathfrak{M}_2 at support B .

The full line and two kinds of dotted line represent the influence line for loading along the outermost side, the innermost side, and the center of the road width respectively.

Regarding the bending moment M_2 , the ordinate for outside loading becomes considerably large owing to curvature in the middle span, while it is comparatively small for inside loading.

So, the one is about twice as large as the other.

However, it may be seen that there is little difference owing to eccentricity of loading so far as the bending moment is concerned.

For the warping moment \mathfrak{M}_2 , the ordinate for outside loading has the opposite sign to corresponding one for inside loading.

The same is also valid for the middle span BC .

This result shows apparently that the warping moment takes the opposite sign due to torque loading in the opposite direction.

Next, the influence lines for bending moment M_y at the middle cross section of the center span are shown in Fig. 7.

There is little radial variation of ordinate owing to eccentricity of loading, and the ordinate for inside loading is little larger than that for outside loading.

The shape of influence lines for bending moment M_y is very similar to that about the straight girder.

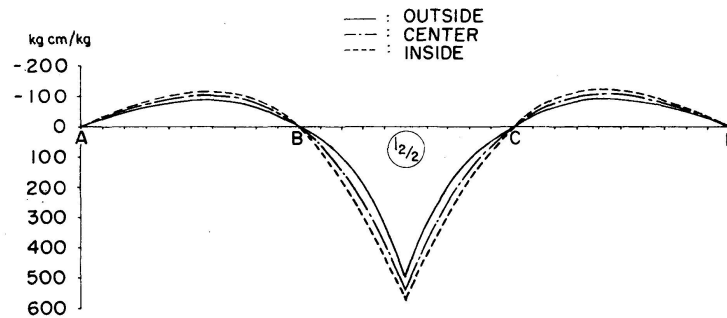


Fig. 7. The influence lines for bending moment $(M_y)_{l_{2/2}}$ at the middle section in the center span.

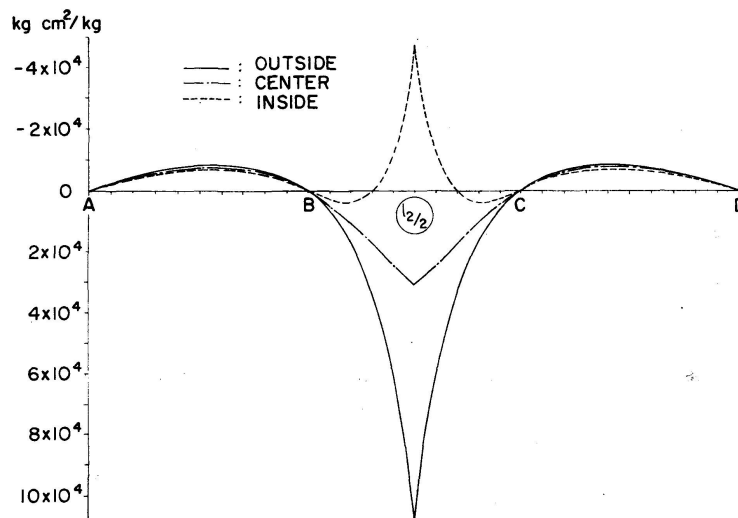


Fig. 8. The influence lines for warping moment $(M_w)_{l_{2/2}}$ at the middle section in the center span.

The influence lines for warping moment M_w at the middle cross section of the center span are shown in Fig. 8.

The ordinate for outside loading is opposite to that for inside loading and the former absolute value is not less than twice as large as the latter in the center span.

On the other hand, there is little effect of radial eccentricity of loading and the absolute value of ordinate is very small all over both side spans.

Therefore, when the secondary normal stress σ_w due to warping moment M_w is superimposed to the primary normal stress σ_b due to bending moment M_y , the total normal stress $\sigma = \sigma_b + \sigma_w$ caused at the cross section of loaded girder becomes larger than that of unloaded girder.

The same fact under the outside loading appears more considerably than that under the inside loading.

Although a load travels along the axis of bridge, the total normal stress in the outside girder is generally larger than that caused at the same time in the inner girder.

This fact is owing to the superposition of two kinds of normal stress. Under non-eccentric loading, the sign of σ_w is the same as that of σ_b in the outside girder, while opposite in the inside girder.

As the stress σ_w can be restricted to fairly small value compared with σ_b value by adopting the closed cross section, the difference between the normal stress σ in the inside girder and that in the outside girder becomes considerably small according to this type of structure.

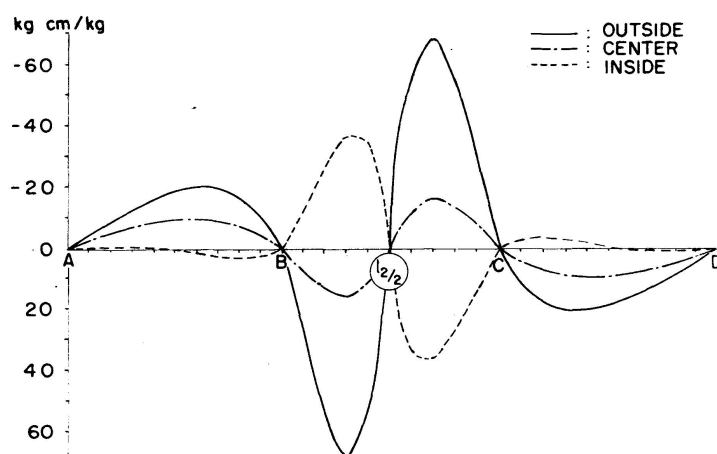


Fig. 9. Influence lines for St-Venant's torsional moment T_s at the middle cross section in the center span.

The influence lines for St-Venant's torsional moment T_s at the middle cross section of the center span are shown in Fig. 9. They are just antisymmetric about the middle span, and the absolute value of its ordinate for the outside loading always is larger than that for the inside loading.

Moreover, it should be noted that considerably large torsional moment T_s would be occurred under the side span loading.

The influence lines for secondary torsional moment T_w at the middle cross section in the center span are shown in Fig. 10.

It is discontinuous at the middle section and antisymmetric about that section.

The ordinate decrease suddenly during travel toward the ends of bridge. This fact shows that the influence of adjacent span may be neglected.

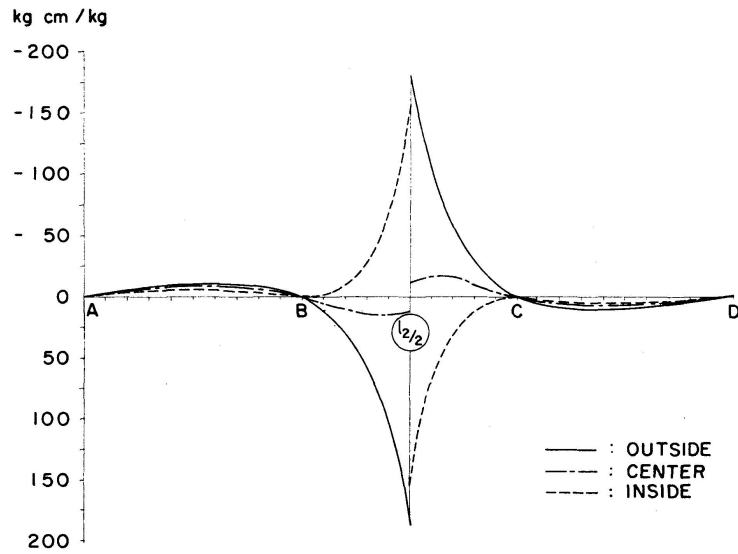


Fig. 10. Influence lines for secondary torsional moment T_w at the middle cross section in the center span.

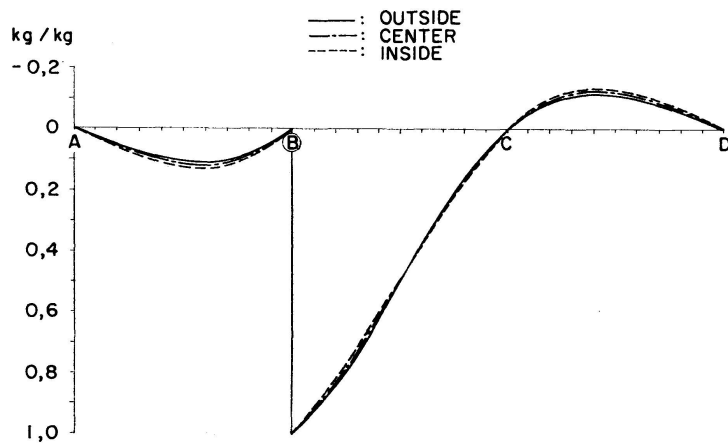


Fig. 11. Influence lines for total shearing force Q at the support B .

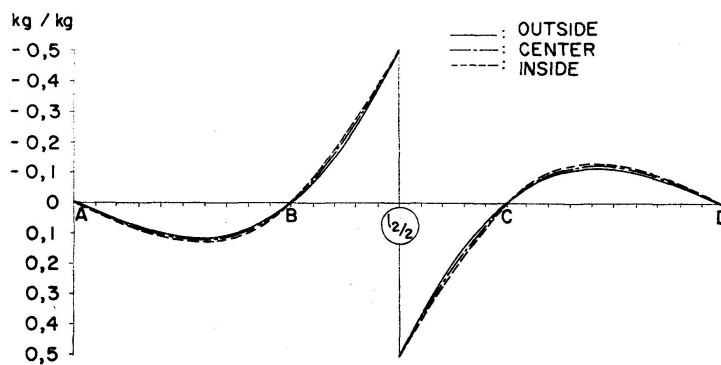


Fig. 12. Influence lines for total shearing force Q at the middle cross section in the center span.

The influence lines for the total shearing force at the support B and at the middle section in the center span are shown in Fig. 11 and 12 respectively.

The effects of both eccentric loading and curvature are scarcely recognized in this example. Then both shape and magnitude are very similar to those of the continuous straight girder.

The influence lines for bending moment M_y at the middle section in the side span are shown in Fig. 13. Respecting the straight side span, it is quite similar to the influence line for bending moment of straight continuous girder.

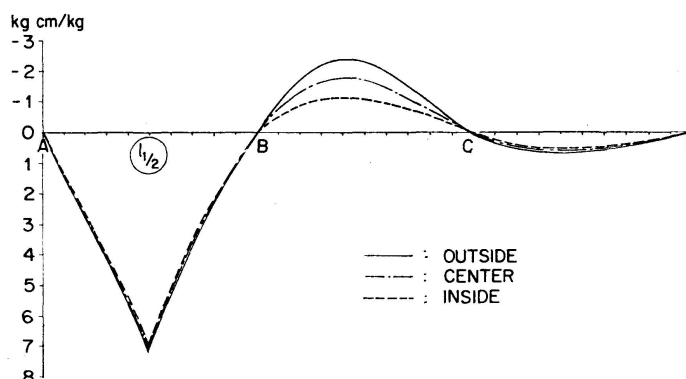


Fig. 13. Influence lines for bending moment M_y at the middle cross section in the side span.

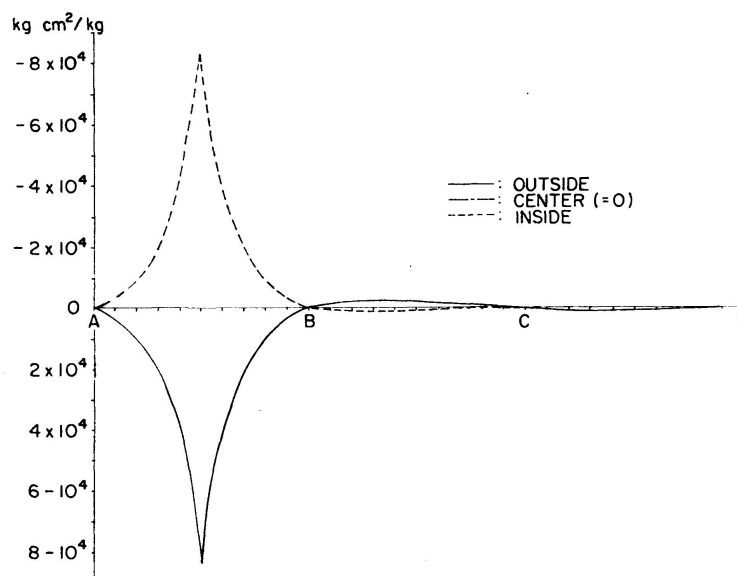


Fig. 14. Influence lines for warping moment M_w at the middle section in the side span.

However, respecting the curved center span, the ordinate for the outside loading becomes larger than that for the inside loading owing to the curvature of bridge axis.

The influence line for warping moment at the middle cross section in the side span are shown in Fig. 14. The value for the outside loading has opposite sign to that for the inside loading and the absolute values for both cases almost are mutually equal.

Those both decrease suddenly according as the load falls away from the

considering section, and that scarcely undergo the influence of loading on the adjacent span. It may be seen that the phenomenon of torsion bending has not been observed under the noneccentric loading. It will be caused by the fact that the considering section lies just in the straight span.

The influence lines for St-Venant's torsional moment and secondary torsional moment at the middle section in the side span are shown in Fig. 15 and 16 respectively.

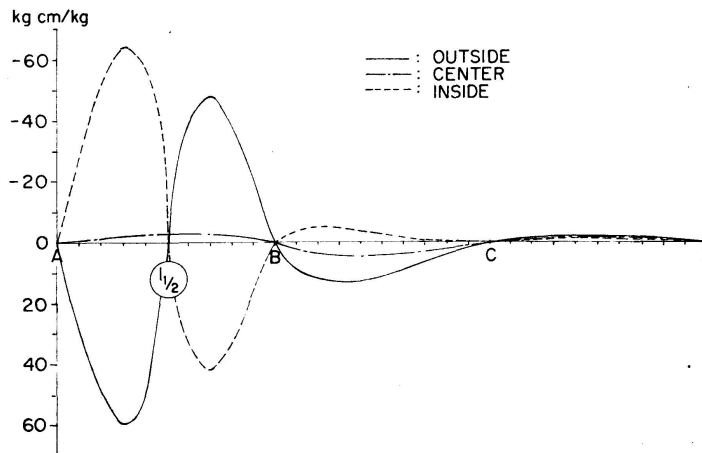


Fig. 15. Influence lines for St-Venant's torsional moment T_s at the middle section in the side span.

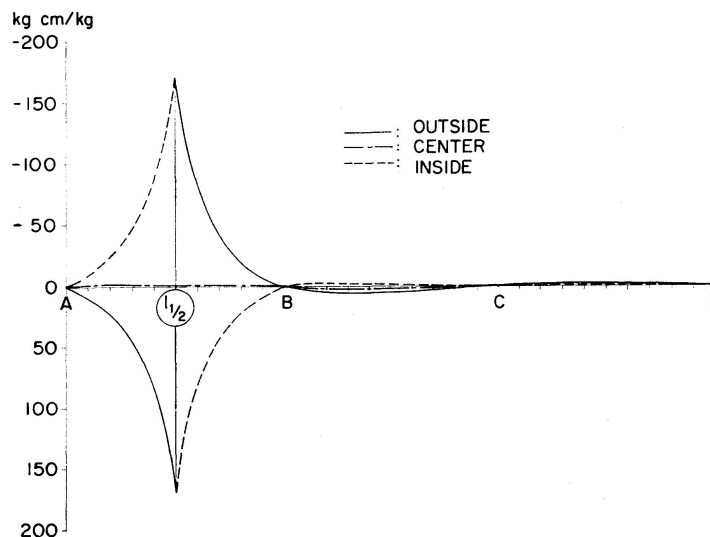


Fig. 16. Influence lines for secondary torsional moment T_w at the middle section in the side span.

In any case, the sign of ordinate converts at the considering middle section. In former case, the absolute maximum value between the middle section and the end support A is greater than that between the middle section and the intermediate support B . This difference is considered to be owing to restraint on warping at the intermediate support B . In latter case, it is much similar

to the influence line for imaginary straight girder, simply supported between two points A and B . The decrement is rapid, so the ordinate in adjacent span is very small.

The influence lines for total shearing force Q at the end section A , the middle section in the side span, and the left side section of support B are shown in

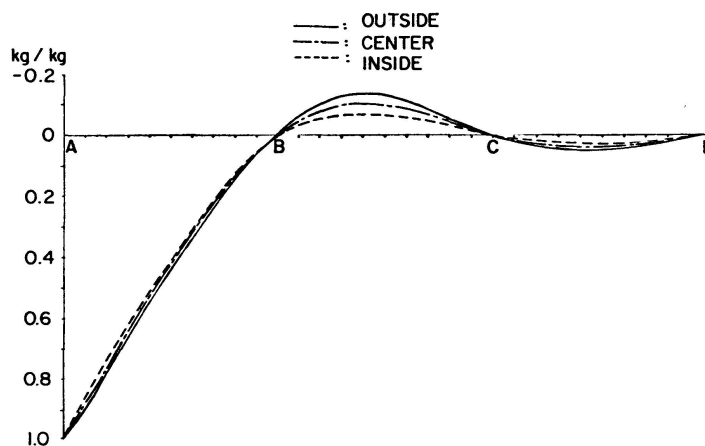


Fig. 17. Influence lines for total shearing force Q at the end cross section A .

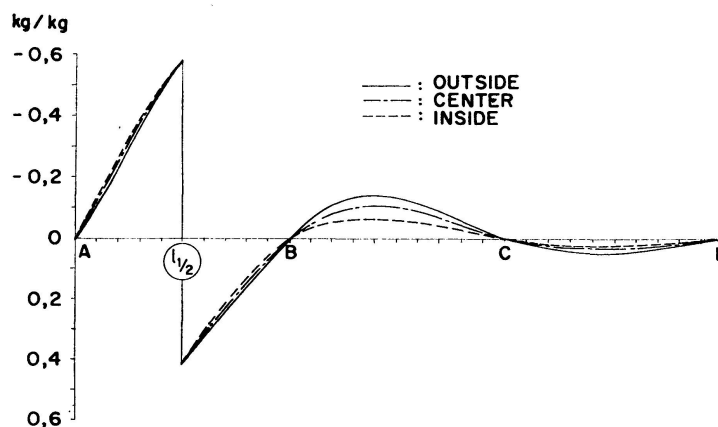


Fig. 18. Influence lines for total shearing force Q at the middle section in the center span.

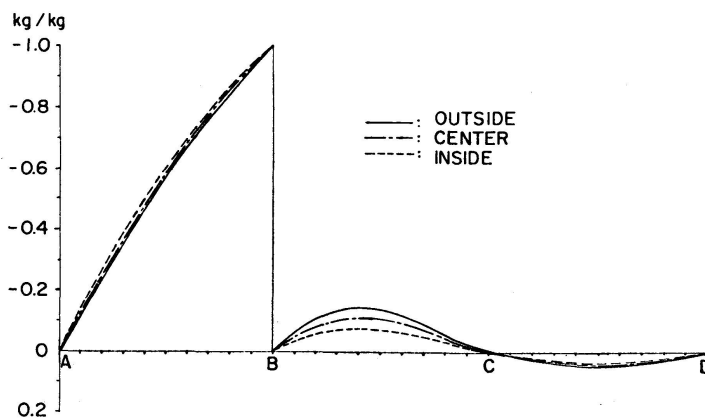


Fig. 19. Influence lines for total shearing force Q at the left side section of support B .

Fig. 17 to 19. In any case, those are much similar to ones for straight continuous girder, while the effect of curvature may be recognized in the center span.

The influence lines for total torsional moment $T = T_s + T_w$ at the middle cross section in the center span and the side span are shown in Fig. 20 and 21 respectively.

In former case, they are just antisymmetric about the considering middle section, and show curvilinear variation unlike the straight continuous girder.

In latter case, they are scarcely differ from those of straight girder, except that little effect of curvature can be recognized in the center span.

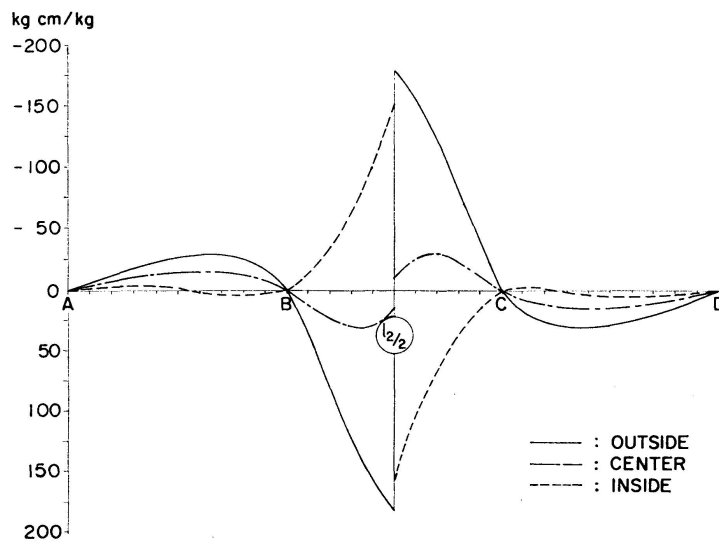


Fig. 20. Influence lines for total torsional moment T at the middle cross section in the center span.

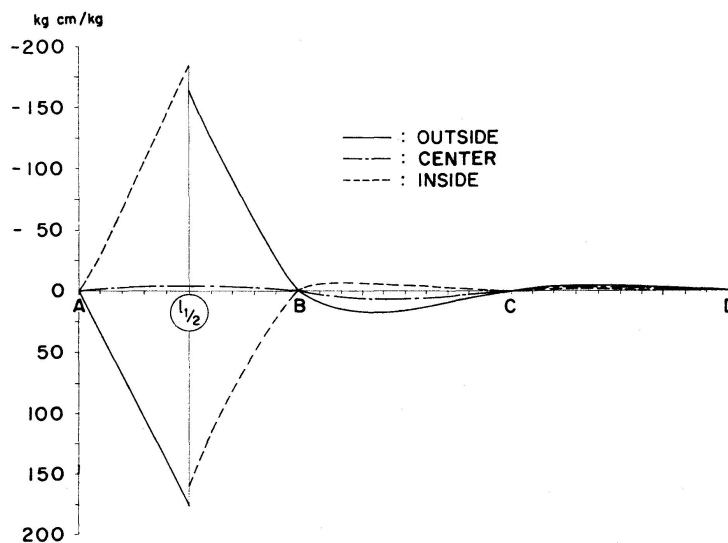


Fig. 21. Influence lines for total torsional moment T at the middle cross section in the side span.

b) Influence Lines for Deformations

The influence lines for deflection δ at the middle cross section in the center span are shown in Fig. 23. They are just symmetric about the middle section. The ordinates for outside loading are about twice as large as those for inside loading.

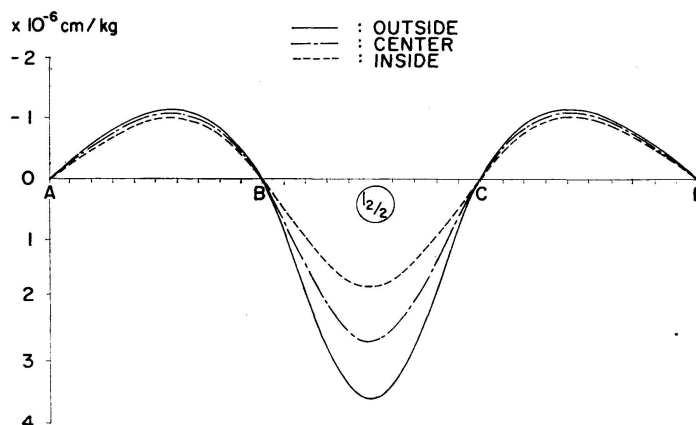


Fig. 22. Influence lines for the deflection δ at the middle cross section of the center span.

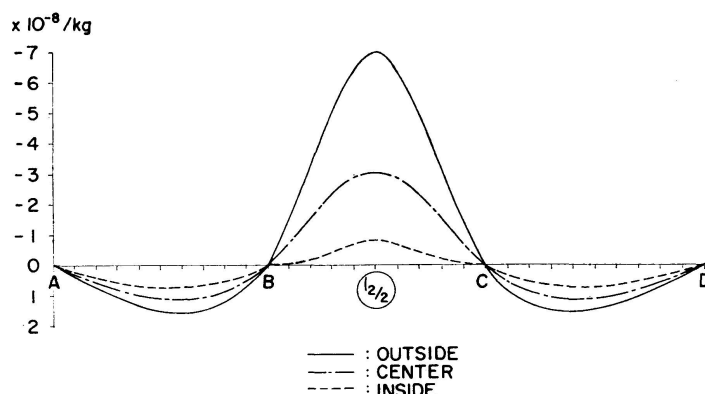


Fig. 23. Influence lines for the angle of rotation β at the middle cross section of the center span.

While the influence lines for angle of rotation β at the same section are shown in Fig. 23. They take negative sign in the center span. These results indicate that the middle section always rotate in the direction that the outside girder have vertical larger displacement than that of inside girder. In the case when the load is placed on the side span, the same section will rotate in the inverse direction. The effect of eccentric loading appears apparently in any case, especially very large rotation is caused by outside loading. It is remarkably characteristic of curved girder bridge with large curvature that the cross-section rotates in the same direction regardless of the radial situation of loading.

References

1. BIEZENO, C. B., GRAMMEL, R.: Technische Dynamik. 2. Auflage, Berlin, 1953, Bd. II.
2. BIEZENO, C. B., GRAMMEL, R.: Engineering Dynamic. 1956, Vol. 2.
3. WANSLEBEN, E. H. F.: Die Theorie der Drillfestigkeit von Stahlbauteilen. 1956, Köln.
4. GOTTFELDT, H.: Die Berechnung räumlich gekrümmter Stahlbrücken. Die Bau-technik, 10. Jahrg., Heft 54, S. 715—724, 1932.
5. VELUTINI, B.: Analysis of Continuous Circular Curved Beams. Jour. ACI, Vol. 22, p. 217—228, 1950.
6. VOLTERRA, E.: Deflections of a Circular Beam out of its Initial Plane. Trans. ASCE, Vol. 120, p. 65—91, 1955.
7. VOLTERRA, E., CHUNG, R.: Constrained Circular Beams on Elastic Foundations. Trans. ASCE, Vol. 120, p. 301—310, 1955.
8. ORAVAS, G.: Beitrag zur Berechnung des Kreisringes auf elastischer Unterlage. Der Bauingenieur, 31. Jahrg., Heft 5, S. 177—180, 1956.
9. FICHEL, H. H.: Analysis of Curved Girders. Proc. ASCE, Vol. 85, No. ST 7, p. 113 to 141, 1959.
10. RESINGER, F., EGGER, H.: Die Kummerbrücke — ein interessantes Kastenverbund-system. Der Bauingenieur, 35. Jahrg., Heft 6, S. 216—222, 1960.

Summary

In this study, the torsion bending theory has been developed into the three dimensional analysis for curved girder, and following general results have been obtained.

1. The various statical quantities related to geometrical factor of cross section have been explicitly defined.

2. Seven fundamental conditions of deformation have been investigated and the relations among the deformation, stress resultants and stress have been made clear with regard to free-free curved girder.

3. The formula which gives the position of shear center has been derived.

4. The relation among the torsional angle, absolutely angle of rotation of whole section and deformation has been obtained.

5. The solutions for stress resultants and deformations have been obtained for both simply supported and continuous curved girder under typical loading conditions.

6. In a numerical example, influence lines for stress resultants and deformations have been found, so that some important statical characteristics of curved girder have been made clear.

Résumé

Les auteurs développent la théorie de la torsion-flexion en l'appliquant à l'étude tridimensionnelle des poutres courbes. Ils présentent les résultats généraux suivants:

1. Ils définissent explicitement les grandeurs statiques relatives aux données géométriques de la section.
2. On étudie sept conditions fondamentales de déformation et, pour la poutre courbe à extrémités libres, on précise les relations entre les déformations, les sollicitations et les contraintes.
3. On établit une formule donnant la position du centre de cisaillement.
4. On déduit la relation liant l'angle de torsion, l'angle de rotation absolu de la section et la déformation.
5. Des solutions pour les sollicitations et les déformations sont obtenues, dans des cas de charge typiques, soit pour des poutres courbes simples, soit pour des poutres continues.
6. Dans une application numérique, on donne des lignes d'influence pour les sollicitations et les déformations; on met ainsi en évidence quelques caractéristiques statiques importantes des poutres courbes.

Zusammenfassung

In dieser Studie wurde die Biege- und Torsionstheorie für die dreidimensionale Untersuchung gekrümmter Träger weiterentwickelt, wobei folgende allgemeine Ergebnisse erzielt wurden:

1. Zuerst werden die verschiedenen statischen Werte im Zusammenhang mit den geometrischen Querschnittsgrößen definiert.
2. Sieben fundamentale Beziehungen für die Verformungen werden untersucht und die Beziehungen zwischen Verformungen, Schnittkräften und Spannungen werden erläutert im Zusammenhang mit einem gekrümmten Träger mit freien Enden.
3. Die Gleichung, welche die Lage des Schubmittelpunktes angibt, wird abgeleitet.
4. Die Beziehung zwischen Torsionsdrehwinkel, absolutem Verdrehungswinkel des Gesamtquerschnitts und Verformung werden angegeben.
5. Die Beziehungen für die Schnittkräfte und die Verformungen werden sowohl für den einfachen als auch den kontinuierlichen gekrümmten Träger für die typischen Belastungsfälle angegeben.
6. In einem numerischen Beispiel werden die Einflußlinien für die Spannungen und für die Verformungen angegeben, so daß einige wichtige statische Eigenschaften gekrümmter Träger klar ersichtlich werden.